Oscillatory Patterns During Emotional Face Processing using OPM-MEG data

Clara Holst (CH), AU737540 (202306022@post.au.dk)

Réka Forgó (RF), AU737257 (202308670@post.au.dk)

Supervisor: Lau Møller Andersen

Bachelor's project

Bachelor in Cognitive Science

School of Communication and Cognition

Faculty of Arts, Aarhus University,

Jens Chr. Skous Vej 2, 8000 Aarhus, Denmark

16/12/2025

Characters: 92.523 ~ 38 pages

Abstract

Human face perception is a rapid, multidimensional process crucial for social interaction. It involves the simultaneous decoding of invariant characteristics, such as race, gender, and age, as well as variable features like emotional expression. Although recent research has begun to map the temporal dynamics of these different dimensions, the underlying oscillatory neural mechanisms, specifically how different brain rhythms interact to facilitate this process, remain poorly understood. Evidence for cross-frequency coupling (CFC) in face perception using non-invasive methods is limited. The strongest direct evidence comes from Furl et al. (2014), who used magnetoencephalography (MEG) data to demonstrate cross-frequency coupling in face-selective brain areas, specifically showing theta power suppression of beta power in the face perception network. However, this research does not differentiate between specific facial dimensions, such as emotional expression, race, gender, or age.

In this project we used the publicly available Optically Pumped Magnetometer MEG (OPM-MEG) dataset by Xu et al. (2024) in which participants viewed faces varying in race, gender, age, and emotional expression. We employ time-frequency analysis and measures of cross-frequency coupling to investigate oscillatory dynamics, focusing on the interplay between theta, alpha, and gamma bands.

We hypothesized that emotional faces would elicit significantly stronger early theta-band power (0-300 ms) over occipitotemporal regions, reflecting the rapid detection of emotional salience. Furthermore, given the role of alpha oscillations in attentional gating and cortical inhibition, we expected that emotionally salient faces, due to their heightened motivational relevance, would engage attentional resources more strongly than neutral faces, leading to greater posterior alpha desynchronization (event-related desynchronization, ERD). We also anticipated observable alpha-gamma and theta-gamma phase-amplitude coupling, a measure of cross-frequency coupling (CFC), over posterior sensors, reflecting increased cortical disinhibition and accelerated feature integration driven by emotion-related attentional engagement. We predicted that variation in alpha band power during emotionally relevant trials would be correlated with faster response times. Finally, as an exploratory aim, we employed machine learning models to determine if oscillatory features from theta and alpha bands could classify emotional faces more accurately than models using traditional event-related potentials.

This study aims to provide a clearer account of the oscillatory mechanisms underpinning emotional face perception and showcases the utility of OPM-MEG for cognitive neuroscience.

Table of Contents

Introduction

1.1. The Social Brain and the Challenge of Face Perception (CH)

Human social life appears to be fundamentally intertwined with our capacity to recognize and interpret faces. A single glance at a face conveys identity, emotional state, intentions, and social information, making face perception one of the most highly developed visual skills in humans (Haxby et al., 2000; Oruc et al., 2019). This ability is so central to survival and communication that it is often described as the front end of the social brain, shaping first impressions and guiding social behavior (Leopold & Rhodes, 2010; Deen et al., 2023).

Neuroimaging and neuropsychological studies reveal that face perception is supported by a distributed neural network comprising both a core system and an extended system. The core system includes the occipital face area (OFA), fusiform face area (FFA), and a face-selective region in the superior temporal sulcus (STS/fSTS). These occipitotemporal regions mediate the structural encoding of faces, with the OFA and STS responding to the presence of facial parts, while the FFA integrates both the parts and their configuration, supporting holistic perception (Kanwisher et al., 1997; Liu et al., 2010).

White-matter tractography further demonstrates strong connectivity between OFA and FFA, particularly in the right hemisphere. This robust anatomical linkage implies a highly efficient and specialized pathway for rapid information transfer, which is essential for integrating facial features into a unified percept within milliseconds. Meanwhile, the STS connects along a more dorsal route with parietal and frontal areas, facilitating the integration of perceptual data with attentional and social-cognitive processes. Early visual cortex also projects directly to the amygdala, underscoring the close coupling of perceptual and affective systems (Gschwind et al., 2012).

The extended system, which includes structures such as the amygdala, hippocampus, and inferior frontal gyrus, integrates the core system's perceptual signals with memory, emotion, and higher-order cognition. These regions link perceptual processing to emotional salience, personal familiarity, and contextual meaning (Haxby et al., 2000; Xu et al., 2024). This interaction explains why facial recognition is disrupted in conditions such as prosopagnosia, where lesions to occipitotemporal regions selectively impair face identity recognition while sparing other visual functions (Kanwisher et al., 1997; Barton, 2008).

Classical cognitive models further illustrate the complexity of face processing. Bruce and Young (1986) proposed that distinct functional codes, including those for identity, expression, speech-related mouth movements, and name retrieval, operate in parallel but interact dynamically. Supporting this, electrophysiological and fast periodic visual stimulation studies show that individual face discrimination can emerge within approximately 170 ms, reflecting the rapid temporal dynamics of the system (Rossion, 2014).

Together, these findings highlight that the challenge of face perception lies not only in identifying where in the brain faces are processed, but in understanding how multiple specialized systems interact within a fraction of a second to transform visual input into socially meaningful information.

1.2. Oscillatory Dynamics as a Key Neural Mechanism (RF)

Brain rhythms, or in other words, oscillations, are time-based changes in excitability of neural populations. They can be described on a neurological (physiological) or a cognitive (functional) level. In this paper we will focus on their functional aspects, but first we want to describe some of the key terms which will be used later in the paper.

Neural rhythmic activity reflects the changes in neuronal excitability, and they regulate the communication in neuronal circuits. They are synaptic interactions among excitatory and inhibitory neurons that form the simplest circuit which generates synchronised oscillations through back-and-forth interactions (Keitel et al., 2025).

Neural oscillations can be quantified by changes in their amplitude (power), frequency or phase and these can be measured best through electrophysiological recording methods, such as EEG, MEG or OPM since these devices have high temporal resolution when recording brain activity. The neuronal activity has to be highly synchronised in a group of neurons to be measurable. Generally speaking, the oscillations are, after recording, filtered to narrow frequency bands or Fourier transformed (Keitel et al., 2025). These frequency bands are traditionally: delta (1-4 Hz), theta (4-8 Hz), alpha (8-14 Hz), beta (14-30 Hz) and gamma (30-120 Hz) (Groppe et al., 2013). It is assumed that these oscillations create a temporal scaffolding for information processing (Buzsáki, 2006). In the light of predictive processing, one theory is that lower-frequency activities tend to carry predictions in feedback directions, while higher-frequency (gamma) activity is associated with prediction errors carried forward (Bastos et al., 2012).

From a functional perspective, changes in phase or power of neural oscillations can often be associated with multiple cognitive functions (Keitel et al., 2025). The mechanisms of oscillatory functions also describe how two different oscillatory cycles relate to each other (one cycle is one peak and one trough). For example two oscillators are considered synchronised when their peaks and troughs align or show statistically significant coupling over time or across trials.

1.2.1. Theta Oscillations in Emotional Salience and Integration (RF)

Theta rhythms are consistently linked to the detection and integration of emotionally salient information. They increase when the visual system encounters affectively significant stimuli (Keitel et al., 2025), and this pattern extends robustly to facial expressions. Theta synchronization differentiates emotional from neutral faces (Symons et al., 2016), with a clear temporal bifurcation: an earlier theta increase (~150-250 ms) reflects the rapid

extraction of emotional salience, while later sustained theta activity relates to integrating sensory input with stored affective or mnemonic representations.

This two-stage profile aligns with Xu et al. (2024), who report that expression is one of the earliest and most stably decodable dimensions, showing a temporally dominant structure beginning around 200 ms and persisting across later windows. Overall, literature positions theta as a rhythm that organizes the earliest stages of affective face perception: rapid salience extraction followed by the integration of emotional meaning with perceptual and mnemonic context. This makes theta a central candidate mechanism for understanding how the brain prioritizes emotionally significant faces.

1.2.2. Alpha Oscillations in Attentional Gating and Inhibition (RF)

Alpha rhythms index inhibitory control and attentional gating. Decreases in alpha power (ERD) signal heightened cortical engagement, particularly in visual areas (Keitel et al. 2025). Emotionally intense stimuli often evoke posterior alpha ERD, a component of emotion perception that appears both across positive and negative images (Güntekin & Basar, 2006). This desynchronization reflects a release of inhibition to permit enhanced sensory processing (Balconi et al., 2009).

Alpha dynamics also reveal multi-stage processing. Popov et al. (2013) describe an initial pattern of increased frontal and sensorimotor alpha with concurrent occipital alpha suppression, interpreted as engagement of control systems followed by perceptual uptake, followed by a reversal during post-recognition stages. Alpha synchronization can further indicate uncertainty resolution or selective inhibition (Symons et al., 2016).

In the context of face processing, the research by Xu et al. (2025) showed sustained discriminability for race and expression perception in later time windows (300-400 ms), consistent with the role of alpha in later evaluative and categorization processes. Moreover, the temporal interactions they identify, for example, expression affecting race processing around 200-300 ms which fits with an alpha-mediated mechanism in which emotional salience modulates attentional gating for other facial dimensions.

Alpha's role in gating sensory inflow and reallocating attentional resources positions it at the interface between perception and evaluation. Emotional expressions often trigger shifts in attentional priority, and alpha rhythms provide a mechanism through which such reallocation can occur, first through rapid inhibition release in posterior cortex, later through adjustments that reflect categorization demands or uncertainty resolution. In this sense, alpha dynamics offer a wider functional window onto how emotional information interacts with concurrent perceptual processes.

1.2.3. Gamma Oscillations and Feature Binding (RF)

Gamma (30-120 Hz) oscillations have been repeatedly linked to visual awareness and feature binding (Keitel et al., 2025). In face perception, gamma activity appears to represent this

binding role along the ventral visual pathway. Yin et al. (2020) report enhanced gamma power and short-range gamma coupling in inferior occipital gyrus, fusiform gyrus and superior temporal sulcus during face versus non-face perception, with additional long-range gamma coupling along right occipito-temporal pathways. Increased gamma band power has been interpreted as reflecting more efficient collection and integration of low-level visual features into higher-order face representations (Keitel et al., 2025). In affective contexts, studies such as Symons et al. (2016) suggest that gamma synchronisation within regions such as the occipito-temporal cortex, orbitofrontal cortex and amygdala facilitates the processing of emotional significance of features in faces.

Rather than indexing a single computational step, gamma appears to coordinate multiple representational stages, from early feature extraction to the amplification of diagnostic affective cues. Framing gamma in this way highlights its role as an integrative rhythm within the broader face-processing architecture and underscores why examining its relation to lower-frequency bands is informative for understanding how perceptual and affective processes interact.

1.3. The Multidimensional Nature of Faces (CH)

Although faces appear to us as unified percepts, they are more likely to be multidimensional stimuli. Each face simultaneously conveys a complex array of information, including relatively stable, invariant characteristics such as race, gender, and age, which aid in identity recognition, and dynamic, variable features such as emotional expression, which signal immediate internal states and intentions (Bruce & Young, 1986; Xu et al., 2024). The human brain is adept at processing these dimensions in parallel, yet they are not created equal; they differ in their neural salience, the speed of their processing, and their susceptibility to experience-based biases (Oruc et al., 2019). While faces simultaneously convey race, gender, age, and expression, this study specifically investigates emotional expression due to its rapid social relevance and distinct neural dynamics.

Facial expressions rapidly convey affective states and intentions, directly influencing social interaction and behavior. At the neural level, oscillatory dynamics are fundamental to this process. A key and consistent finding is that emotional expressions, whether pleasant or unpleasant, prompt enhanced theta-band synchronization (≈150-250 ms) compared to neutral faces, facilitating the rapid encoding of emotionally salient sensory information over distributed ventral visual, parietal, and anterior hippocampal regions (Balconi & Lucchiari, 2006; Symons et al., 2016). This early theta response is thought to reflect the orienting of attention toward emotional significance.

Later in the processing stream, gamma-band oscillations are stronger for affective, particularly angry, compared to neutral faces, likely reflecting the facilitated perceptual processing and sensory binding of complex emotional features (Symons et al., 2016). In contrast, the role of alpha oscillations is more nuanced; while emotional images generally

cause alpha desynchronization (ERD) over posterior sensors, indicating increased cortical excitability, effects with static faces are less consistent and may be more tied to selective attention and the motivational relevance of the stimulus rather than pure emotion processing (Codispoti et al., 2023; Campagnoli et al., 2019). This rapid, multi-frequency orchestration allows for the detailed analysis and integration of affective cues, underpinning adaptive social responses.

Finally and most importantly, emotional expression rapidly engages a network of oscillatory rhythms, with theta synchronization (150-250 ms) supporting initial salience encoding and later gamma synchronization reflecting the detailed binding of emotional features (Balconi & Lucchiari, 2006; Symons et al., 2016). Alpha-band activity in this context is more variably involved, often indexing attentional allocation to motivationally significant cues rather than emotion-specific processing (Codispoti et al., 2023).

1.4. Cross-Frequency Coupling: A Framework for Neural Interaction (RF)

Cross-frequency coupling (CFC) provides a critical mechanism for understanding how the brain integrates information across temporal and spatial scales. Rather than examining oscillatory activity within a single frequency band, CFC focuses on the dynamic interactions between distinct rhythms, such as the modulation of high-frequency amplitude (e.g., gamma) by the phase of low-frequency oscillations (e.g., theta or alpha).

In this view, oscillations such as alpha do not merely fluctuate in power but define periodic windows of relative inhibition and excitation. Entering the excitable phase of the alpha cycle releases neuronal populations from inhibition, allowing sequential activation patterns to emerge as bursts of for example gamma activity (Keitel et al., 2025). This is consistent with models such as duty-cycle coding (Jensen et al., 2014), where gamma cycles nested within alpha intervals represent perceptual steps, and with evidence that gamma reflects the activation of feature-specific neuronal assemblies during these high-excitability windows (Montemurro et al., 2008). Cross-frequency coupling could provide a mechanistic account of how low-frequency phase can structure high-frequency content, enabling hierarchical coordination of local and distributed processes relevant to perception and cognition.

This hierarchical coordination also allows for the binding of local and distributed neural processes, enabling efficient communication between cortical regions during complex cognitive tasks (Canolty & Knight, 2010; Aru et al., 2015). In the context of face perception, cross-frequency coupling may reflect the integration of sensory encoding and higher-order evaluative processes, linking early visual analysis with emotional and mnemonic networks. OPM-MEG, with its superior signal sensitivity and spatial precision, offers a great potential platform for capturing cross-frequency interactions. By applying metrics such as Phase-Amplitude Coupling (PAC) and related decomposition methods, this study aims to quantify how oscillatory hierarchies coordinate the temporal evolution of face processing in the human brain.

However, it is important to note that there is a reason why there are currently only a few studies in this area. The reason for that is the presence of the zero-lag effect, especially in electrophysiological studies, where a signal is picked up by all sensors, and not just ones in the observed area. Hence, when analysing CFC often we can get spurious results, since the signal propagates to all sensors, instead of just one (Keitel et al., 2025). In our study, we aim to explore cross-frequency coupling as a method, but it is not the main point of our research.

1.5. Advancing the Field: OPM-MEG and Multivariate Decoding (CH)

This research leverages the significant technological advantages of Optically Pumped Magnetometer-based Magnetoencephalography (OPM-MEG) to address longstanding questions about the rapid neural dynamics of face processing. Conventional magnetoencephalography (MEG) systems use Superconducting Quantum Interference Devices (SQUIDs), which require cryogenic cooling and a fixed, one-size-fits-all helmet. This design limits participant mobility, creates a distance between the sensors and the scalp, and attenuates high-frequency neural signals.

In contrast, OPM-MEG utilizes compact, laser-pumped atomic magnetometers that operate at room or body temperature (Boto et al., 2018). This fundamental difference enables a "wearable" system where lightweight sensors can be placed directly on the participant's scalp in a customized array, dramatically reducing the brain-sensor distance. The technical benefits of this approach are profound. First, the reduced distance and novel sensor design increase both signal strength and signal-to-noise ratio to some cortical sources (Iivanainen et al., 2017) and to higher-frequency neural signals like gamma oscillations (30-120 Hz). Gamma activity is crucial for cognitive processes such as feature binding but is often poorly captured by conventional SQUID-MEG (Hill et al., 2021). Second, the system is motion-robust, allowing for natural head movements during recordings. This improves participant comfort, reduces motion-related artifacts, and enables more ecologically valid experimental paradigms (Tierney et al., 2021). Additionally, OPM arrays can be adapted to any head size, ensuring optimal sensor positioning across diverse populations (Seymour et al., 2022). Finally, the critical advantage is reduced sensor-to-scalp distance, which increases signal amplitude, particularly for high-frequency gamma oscillations crucial for feature binding, and allows for motion-robust, more naturalistic paradigms.

1.6. Research Gaps (CH)

Despite these advances, several critical gaps persist. First, although distinct roles for theta, alpha, and gamma oscillations in face perception have been proposed (Keitel et al., 2025), their dynamic interaction, particularly via cross-frequency coupling (CFC), during the rapid and parallel processing of facial and emotional dimensions remains largely unexplored with non-invasive methods (Yin et al., 2020). Existing evidence has predominantly focused on power changes within isolated frequency bands (Keitel et al., 2025), leaving open the

question of whether oscillatory interactions provide a richer neural signature of face and emotion processing than traditional event-related potentials. Furthermore, the relationship between trial-by-trial fluctuations in oscillatory activity and behavioral performance is poorly characterized. Moreover, progress has been limited by methodological challenges, including the susceptibility of CFC metrics to artefacts such as volume conduction, which complicates interpretation at the sensor level (Young & Eggermont, 2009).

Second, the oscillatory signatures specific to emotional expression processing, as distinct from other, consistent facial features like identity or race, require clearer differentiation (Sauseng & Klimesch, 2009). Although enhanced theta synchronization to emotional faces is a consistent finding, the evidence for emotion-specific modulation of alpha rhythms is mixed and may depend on stimulus properties and task demands. Furthermore, it is unknown whether the neural code for emotional expression is better captured by traditional event-related potentials or by sustained oscillatory features, a question with direct implications for developing neural biomarkers and brain-computer interfaces. Time-resolved analyses increasingly suggest that ERPs alone cannot capture the full temporal structure of face-related information (Xu et al., 2024 ; Rossion & Retter, 2015).

A further gap concerns the link between oscillatory activity and behavior: only a few studies examine how trial-by-trial fluctuations in rhythms such as alpha desynchronization, and the associated changes in excitability and attentional gating, relate to performance or decision speed (Keitel et al., 2025; Young & Eggermont, 2009).

Finally, the technological limitations of conventional neuroimaging have long constrained this line of research. Traditional MEG systems, for example, have reduced sensitivity to high-frequency gamma oscillations and restrict naturalistic experimental paradigms. The recent development of Optically Pumped Magnetometer (OPM) MEG offers a promising solution (e.g., Xu et al., 2024). OPM-MEG provides higher signal strength, improved signal-to-noise ratio, enhanced sensitivity to high-frequency activity, and, in some cases, tolerance to participant movement, allowing for precise measurement of the brain's full oscillatory repertoire in more naturalistic settings.

This study aims to bridge these gaps by leveraging a publicly available OPM-MEG dataset (Xu et al., 2024). We will investigate the oscillatory dynamics underpinning emotional face perception by testing for early theta power increase as a marker of emotional salience; examining whether emotional expressions produce distinct alpha-band desynchronization and low-phase/ high-amplitude cross-frequency coupling patterns; linking oscillatory measures to behavioral performance; and directly comparing the predictive power of oscillatory features against traditional ERP features for classifying emotional states. This approach allows us to investigate the coordinated oscillatory mechanisms that support the rapid perception of emotional faces.

1.7. Hypotheses (RF, CH)

H1: Theta-Band Power and Emotional Salience

We hypothesize that emotional faces will elicit greater theta-band (4-8 Hz) oscillatory power than neutral faces within early post-stimulus intervals (100-300 ms), maximal over occipitotemporal sensors. This will be tested using one-tailed paired t-tests on three a priori time windows (early: 100-200 ms; mid: 200-300 ms; late: 300-400 ms) and validated with a spatio-temporal cluster-based permutation test to control for multiple comparisons across sensors and time. If confirmed, this would indicate that early theta oscillations serve as a neural marker of rapid emotional salience detection.

H2: Alpha Event Related Desynchronization and Cross-Frequency Coupling

We expect two key outcomes. If emotional expressions do recruit greater attentional gating, conceptualized in the alpha literature as enhanced release of inhibition (Keitel et al., 2025), the expected outcome is stronger posterior alpha (8-12 Hz) desynchronization (i.e., a larger reduction in alpha power relative to baseline) for emotional relative to neutral conditions. Second, on an exploratory basis, we hypothesize that emotional faces will enhance cross-frequency, phase–amplitude coupling (PAC) between low-frequency (theta/alpha) phases and gamma-band amplitude over posterior sensors, consistent with the idea that emotional salience strengthens the hierarchical oscillatory coupling that supports coordinated information flow between integrative and feature-selective neural processes.

H3: Behavioral Correlation with Alpha Dynamics

We predict that the trial-by-trial magnitude of posterior alpha ERD will be negatively correlated with response times in the one-back task, such that greater desynchronization corresponds to faster responses. This relationship will be tested using a linear mixed-effects model. We further predict that this association will be stronger for emotional trials, which will be examined via an interaction term between alpha ERD and emotion condition. If these predictions hold, it would imply that posterior alpha desynchronization reflects task-relevant fluctuations in cortical excitability that directly shape behavioral efficiency, and that emotional expressions strengthen this excitability-behavior link.

H4: Machine Learning Classification

We hypothesize that machine learning models using oscillatory power features (from theta and alpha bands) will classify emotional versus neutral faces with greater accuracy than models using traditional event-related potential (ERP) features. Superior performance will be defined as a significantly higher mean Area Under the Curve (AUC) across participants, assessed with a paired-sample t-test. If confirmed, this would indicate that oscillatory features provide a more informative and functionally relevant neural signature of emotional face processing than conventional ERP measures.

Methods

2.1. Dataset Description (Xu et al., 2024) (RF)

Data was acquired from *openneuro.com*, under the name FACE-DEC by Xue et al., 2024. Theirs was an OPM-MEG study designed to characterize the temporal structure of race, gender, age, and expression dimensions during face processing. Recordings were acquired using a scalp-mounted OPM-MEG array. Each participant completed multiple runs of a rapid one-back face task in which artificially generated faces (manipulated across four binary dimensions) were presented, followed by a fixation interval.

2.1.1. Participants (CH)

23 right-handed Chinese participants were recruited for the experiment. Two were excluded as they reported difficulty staying still during the recording. Standard OPM MEG enables slight movement to be possible without generating excessive noise in the data, but in this particular example, the setup did not allow for as free movement as normal. Data from the remaining 21 participants (10 females; 11 males; between ages 21 - 28, (mean age = 22.29, SD=2.12 years)) were included in the analyses. All participants had normal or corrected-to-normal vision and were not aware of the purpose of this study. None reported a history of neurological or psychiatric symptoms. Participants were compensated for their time, and this study was approved by the Institutional Review Board of Peking University (Xu et al., 2024).

2.1.2. Stimuli and Experimental Design (RF)

In the experiment (Xu et. al, 2024) stimuli were generated using a StyleGAN2 (Style-based Generative Adversarial Network, by NVIDIA Research (Karras et al., 2019)) model and were created across race (Asian/Caucasian), gender (female/male), age (young/elderly), and expression (neutral/joyful). For the sixteen unique combinations, four exemplars for each were created (64 total). Stimuli were normalized for luminance, root mean square (RMS) contrast, facial position, and size. All images were embedded in scrambled backgrounds to suppress low-level confounds (Appendix 1)**.** Each trial consisted of a 200-ms face presentation followed by a 900-1100-ms fixation cross interval. Fixation interval length was randomised to prevent predictability effects. Participants performed a one-back repetition detection task, meaning their task was to identify if a face is one that they have seen just before (catch trials). For each run (lasting around 5-6 minutes) participants were shown all 64 different faces four times, along with 14 catch trials. Participants were instructed to react to these catch trials with a button press. Trial order was pseudorandomized, and catch trials were inserted in an unpredictable but uniform manner to prevent repeated button presses (Xu et al., 2024). Participants completed two sessions separated by a 1-hour break, producing ~20 runs of data per participant. Behavioral performance was stable according to Xu et al. (2024) (mean $RT \approx 557$ ms).

2.1.3. Experimental system (RF)

Recordings were conducted with using an OPM-MEG system and a setup designed by the experimenters (Xu et al. 2024) where they placed sensors close to the scalp and covered with thin layer of gel for insulation, then participants lied down in the cylindrical shield (PyraMag Epoch 64 OPM-MEG system (Quanmag Healthcare)). The data was collected when participants were lying down. See figure 1 below, which was produced by experimenters on experiment setup. Data was recorded at a sampling rate of 1,000 Hz with a 24-bit digital acquisition system (Quanmag Healthcare).

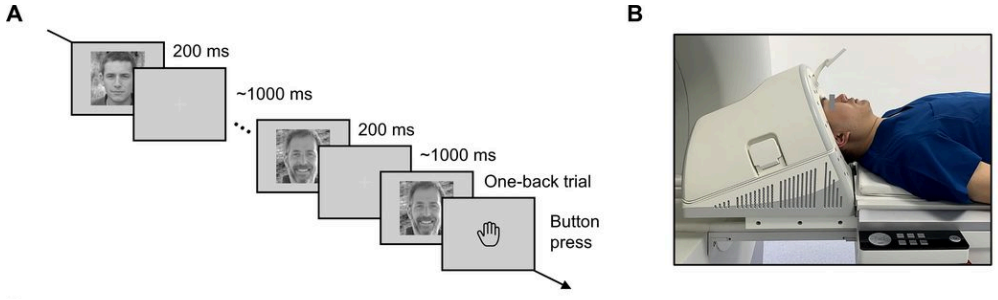

Figure 1: Figure produced by Xu et al., (2024). A) is experiment design, B) scanning position.

There were no individual headshape digitalisation files recorded, nor structural MRI scans, as this technology was not available to the researchers at the time of the recording. Furthermore there were neither electrooculography (EOG) channels to monitor eye blinks and movements nor electrocardiogram (ECG) to monitor heart rate. It should also be noted that the sensor coordinates were approximated by selecting corresponding locations from the Elekta layout and do not reflect the actual, precise sensor positions (Xu et al. 2024)

More detailed description about experiment setup and data acquisition can be read in Xu et al., 2024.

2.2. Data Preprocessing (RF)

All preprocessing was conducted using MNE-Python (v1.10.2; Gramfort et al., 2013) together with custom Python scripts. Data preprocessing steps included marking noisy and flat channels, notch and band-pass filtering, epoching the data based on events, marking and dropping bad epochs (Ferrante et al., 2022).

First of all, raw data was loaded in, then power spectral densities (0.1-150 Hz, Welch method) were computed for all channels. Channels whose broadband power exceeded four times the subject-specific median total power were labelled as noisy outliers. Channels showing near-zero variance (std < 1×10^{-12}) were labelled as flat/dead. On average this meant keeping around 50.7 ± 1.3 per subject (Figure 2).

For evoked analysis, notch filtering was implemented using a windowed-sinc FIR band-stop filter, applied at line noise frequencies (50 Hz and its harmonics) as well as at 44 Hz, which was reportedly recording equipment noise (Xu et al. 2024). This filtering was applied in a one-pass, zero-phase, non-causal manner to avoid phase distortions. Then another standard FIR band-pass filter (0.1-100 Hz) with symmetric 0.5 Hz transition widths was then applied using the same design constraints (Figure 2).

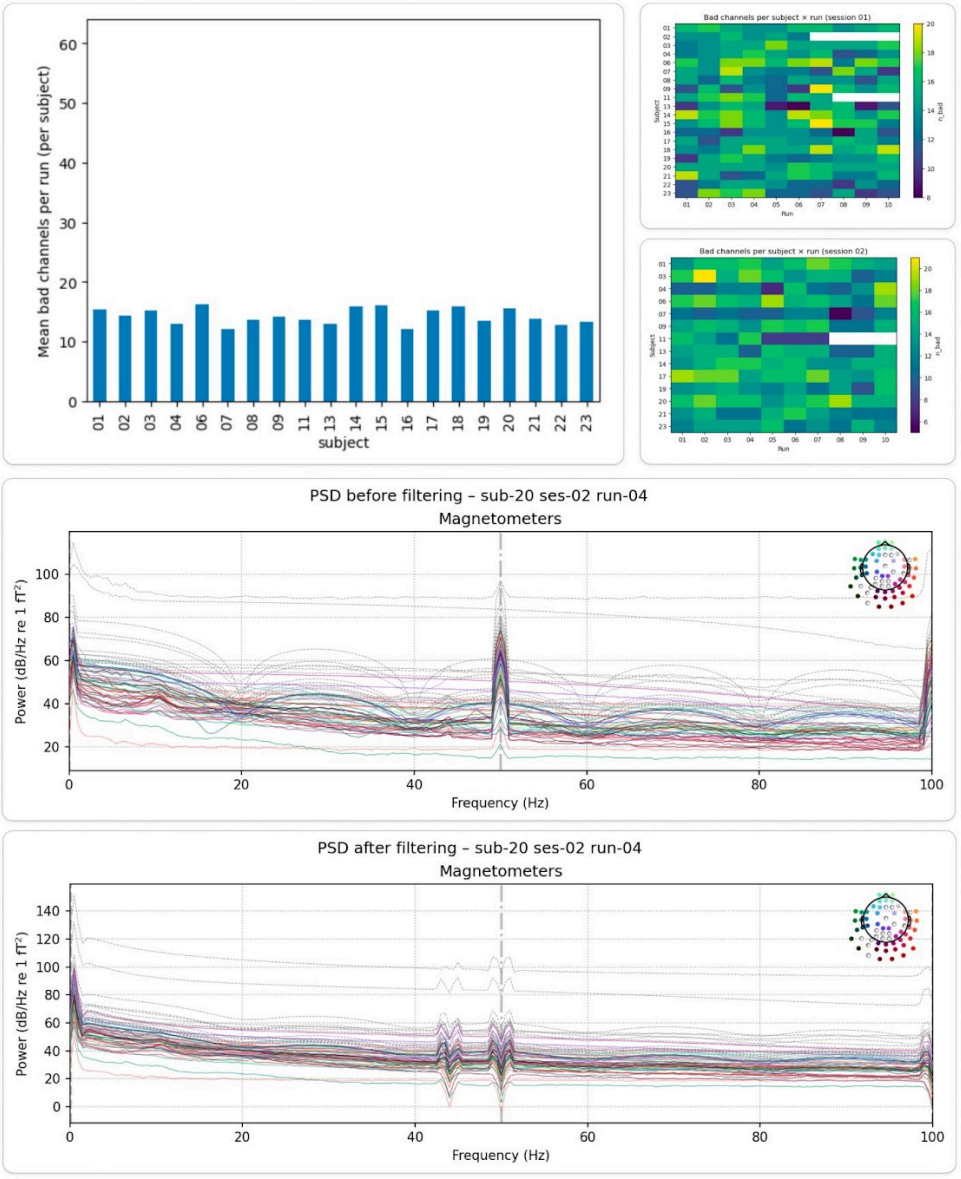

Figure 2: *A) Bad channels per subject on average, (B) and with a matrix per run per session. C) Power spectral densities before and after filtering (See more in the Appendix).*

Even though independent component analysis is a frequently used pre-processing step when it comes to our kind of data, we did not run ICA for multiple reasons. First of all, the absence of EOG/ECG channels and recent literature discussing electrophysiological data preprocessing (Delorme, 2023) lead us to believe that ICA is not the most optimal approach and has limited benefits for statistical power.

Event information was reconstructed by integrating the trigger channel (STIM) with the corresponding behavioral files. A metadata table was created by matching events in the recording to the behavioural information of trial image, which was mapped onto the appropriate conditions. This way the final metadata table contained 4 columns, and within each column a 1 or a 2 indicating the 2 conditions (for example in the "emotion" column 1 = neutral, 2 = joyful stimulus). This made it possible to compare and average trials over the different conditions (see per condition epoch counts in Appendix 5). All one-back trials were excluded for the main analysis.

Epochs were extracted from -200 ms to +800 ms relative to stimulus onset, with a baseline correction interval of -200 to 0 ms. A latency correction of 33 ms was applied to event timings to account for projector delay as reported by Xu et al. (2024). Bad-epoch detection relied on simple, data-driven statistics computed per channel and per epoch. For each epoch, the peak-to-peak (*ptp*) amplitude was computed separately for every MEG channel. This produced a matrix of shape epochs × channels, where each entry quantified the maximum excursion of a sensor within that trial. For each channel, a distribution of peak-to-peak values across all epochs was obtained. The channel-wise mean and standard deviation of these *ptp* values were used to derive a conservative, fixed threshold of 5 standard deviations from the mean. (MNE Python).

This threshold provides a simple estimate of the "normal operating range" of that sensor within the run. An epoch was marked as bad if any of its MEG channels exceeded its channel-specific threshold. This logic captures both global artifacts (e.g., whole-head movement spikes) and focal channel bursts, without depending on hand-tuned per-subject parameters. The total number of epochs was around *86402*, out of which *1644* were dropped. See figure for average epochs dropped by subject (Figure 3). This is minimal data loss. The signal-to-noise ratio after preprocessing was *1.6*, meaning good quality signal across epochs, with a SD of *0.07*.

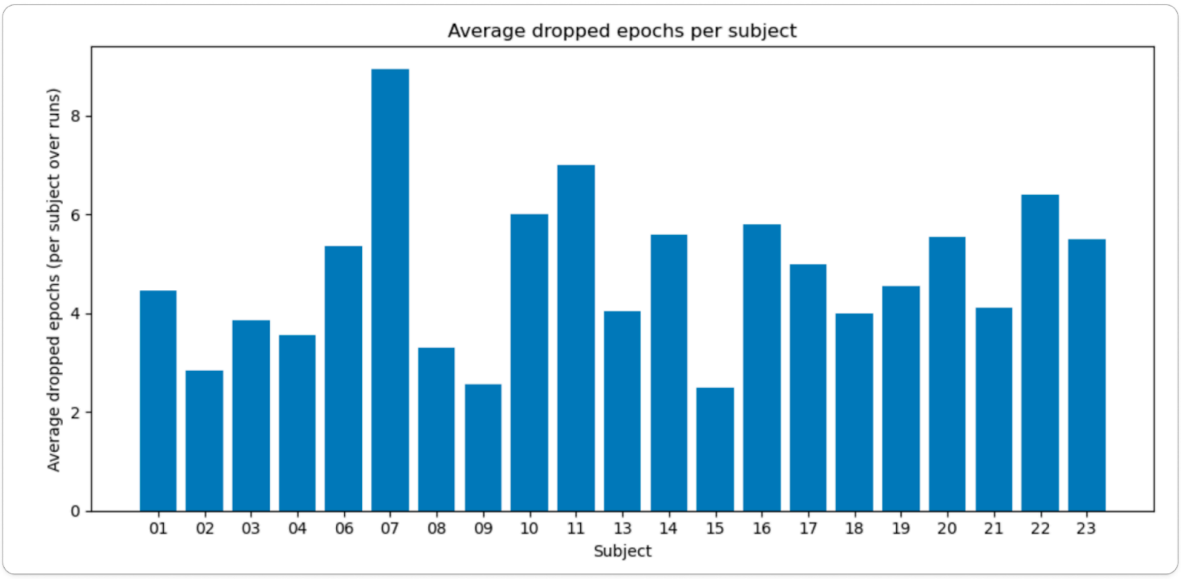

Figure 3: *Average number of epochs dropped per subject (over runs and sessions)*

2.3. Analysis methods (RF, CH)

Primarily libraries used for analysis were MNE Python (v.1.10.2), scikit-learn (v1.3.0, Pedregosa et al., 2011) for machine-learning components and PyTorch (v2.0.0, Paszke et al., 2019) for deep-learning analyses.

Analysis Methods H1 (CH):
Theta band oscillatory power analysis was conducted to test the hypothesis that emotional faces elicit enhanced neural activity compared to neutral faces within early post-stimulus intervals. Theta band power in the 4 to 8 Hz frequency range was extracted using a time frequency decomposition approach. Specifically, we employed Morlet wavelet convolution implemented via MNE Python's tfr_array_morlet function. This method utilized frequency adaptive wavelet cycles, defined as n_cycles = freqs / 3, applied across the theta frequency spectrum. The resulting time frequency representations for each trial were subsequently averaged across the theta frequencies to yield a single power estimate within the theta band for each time point.

Post stimulus power was normalized relative to a pre-stimulus baseline period using a decibel transformation applied correctly in the power domain. The formula power_dB = 10 × $\log_{10}$(power ÷ mean_baseline_power) was used, where mean_baseline_power was computed as the average power during the 200 milliseconds preceding stimulus onset, specifically from 200 to 0 ms. This method properly accounts for baseline activity by expressing post stimulus power as a ratio relative to the pre stimulus mean.

The analysis focused on a predefined region of interest encompassing posterior occipitotemporal sensors. For each participant, condition specific power was first averaged across trials for the emotional and neutral conditions separately. Difference waves were then computed by subtracting the neutral condition power from the emotional condition power for each sensor and time point. These difference values were subsequently averaged across the defined posterior sensor group for further statistical testing. To ensure consistent sensor selection across participants, the intersection of available posterior sensors present in all subjects was used for analysis.

Statistical evaluation employed two complementary approaches. First, planned comparisons were conducted within three a priori time windows: an early window (100 to 200 ms), a mid window (200 to 300 ms), and a late window (300 to 400 ms). For each window, the theta power difference was averaged across the posterior sensors and across the time points within the window. These subject level averages were then submitted to one tailed, one sample t tests against zero, corresponding to the directional prediction that emotional faces would elicit greater theta power than neutral faces. Effect sizes for these comparisons were calculated as Cohen's d, and 95 percent confidence intervals were derived from the standard error.

Second, to address the multiple comparisons problem inherent in testing all sensors and time points, a nonparametric cluster based permutation test was performed. This test, following the methodology of Maris and Oostenveld (2007), was applied to the 100 to 400 ms post stimulus interval. The test procedure involved computing a one sample t statistic at each sensor time point, thresholding these statistics at $t > 2.0$ to form potential clusters of adjacent points in space and time, and calculating a cluster level statistic defined as the sum of the t values within each cluster (cluster mass). To evaluate significance, the condition labels were randomly permuted 1000 times to build a null distribution of the maximum cluster mass. The p value for each observed cluster was then derived by comparing its mass to this permutation based null distribution, thereby controlling the family wise error rate across the entire spatiotemporal search space.

Complementary analyses examined individual variability in response patterns. Individual participant differences were computed as the mean theta power difference across the 100 to 400 ms interval, and the distribution of these differences was assessed for normality using the Shapiro Wilk test. Descriptive statistics including the number of participants showing positive versus negative effects, mean plus or minus standard error of the mean, and 95 percent confidence intervals were calculated.

All analyses were implemented in Python 3.10 using the MNE Python library for core signal processing and statistical functions, with SciPy and NumPy supporting numerical computations, and Matplotlib and Seaborn utilized for data visualization. This analytical framework was designed specifically to test predictions concerning theta band oscillations, excluding other frequency bands to maintain a focused test of the stated hypothesis.

Analysis Methods H2 (RF):

Alpha-band event related desynchronisation (ERD) was quantified from time-frequency representations computed using multitaper decompositions over posterior MEG sensors. Power estimates were extracted in the 8-12 Hz range for each trial and subject and baseline-normalised using a -200-0 ms pre-stimulus interval. Emotional and neutral trials were processed identically. For each subject, alpha power was averaged across the 11 posterior channels (See list in Appendix 3), producing time-bound ERD curves per condition as well as an emotion-neutral difference. Group-level summaries were obtained by averaging these subject-level time courses and by computing paired-sample t-statistics on the condition differences. Time-frequency contrasts were generated by subtracting neutral from emotional power at each time-frequency point. Individual-subject ERD trajectories were retained to allow inspection of consistency and variance across the sample.

Phase–amplitude coupling (PAC) was quantified between low-frequency phase (theta: 4-8 Hz; alpha: 8-12 Hz) and lower gamma-band amplitude (30-40 Hz) over the posterior region of interest (Appendix 3). For each subject, usable channels were determined as the intersection of good channels across all runs, restricted to a predefined posterior sensor list. PAC was computed on epochs from 100-400 ms post-stimulus. Time–frequency

decomposition was performed using Morlet wavelets (MNE tfr_array_morlet). Instantaneous phase was extracted from the complex-valued output for the theta- and alpha-frequency ranges, and gamma-band amplitude was obtained from the magnitude of the 30-40 Hz wavelet coefficients. Phase and amplitude values were averaged across frequencies within each band.

Coupling strength was estimated using the mean vector length (MVL), defined as the magnitude of the average complex vector $A(t)e^{i\phi(t)}$, where where $A(t)$ is the instantaneous gamma-band amplitude and $\phi(t)$ is the instantaneous low-frequency phase across channels, time points, and trials. To assess whether observed PAC exceeded chance expectations, surrogate distributions were generated by circularly shifting the gamma-band amplitude time series by a random temporal offset independently for each trial, preserving both spectral structure and temporal autocorrelation, while destroying the phase–amplitude relationship (Aru et al., 2015). In total, 200 surrogate iterations were computed per subject and condition, and surrogate-normalized scores (*z*-scores) were derived.

Group-level statistical inference was performed on these surrogate-normalized *z*-scores. One-sample t-tests assessed whether mean z-scores differed from zero (i.e., whether PAC exceeded the surrogate baseline). Condition differences (emotional vs. neutral faces) were tested using paired t-tests on the observed PAC values. Cohen's d was used to estimate effect sizes for paired comparisons.

Analysis Methods H3 (RF):

Since behavioural response times were only recorded for one-back trials, epochs were extracted from the preprocessed data, filtered to include only one-back trials with valid responses. A total of 4,014 trials were included (21 participants, mean 191 trials per participant, range 68-258).

Time-frequency decomposition was performed using the multitaper method on the 11 posterior channels (Appendix 3) in the alpha band (8-12 Hz) with frequency-dependent cycles ($n_{cycles} = freq / 2$). Alpha event-related desynchronization (ERD) was computed as percent change from baseline (-200 to 0 ms) and averaged across frequencies, channels, and time points for each trial.

Trial counts were equalised across emotion conditions within each participant to control for possible imbalances. Response time showed a right-skewed distribution and was therefore log transformed prior to analysis. Then linear mixed-effects models were fitted using restricted maximum likelihood (REML) estimation.

Analysis Methods H4 (CH):

To test the hypothesis that oscillatory features provide superior information for emotion classification compared to traditional event-related potentials (ERPs), a comprehensive machine learning pipeline was implemented. Neural data from preprocessed epochs for emotional (joyful) and neutral face conditions were used. For each participant, trials were

first balanced across conditions to ensure equal representation, followed by a final visual inspection of epochs to exclude any residual artifacts.

All 64 OPM-MEG sensors (see Appendix 3) were grouped into four functional-anatomical regions based on their positions relative to standard head geometry. Since individual structural MRIs were not available for this dataset, sensor positions were approximated from the Elekta Neuromag layout as described in Xu et al. (2024). A core set of 24 posterior channels formed the basis for occipital and temporal regions. These were algorithmically divided: approximately 60% (14 channels) were assigned to an Occipital region and 40% (10 channels) to a Temporal region. The remaining 37 non-posterior channels were then distributed between Parietal (19 channels) and Frontal (18 channels) regions based on their numerical sequence and approximate scalp coverage. This comprehensive channel utilization ensured that subsequent analyses captured neural activity across the entire sensor array.

First and foremost, ERP Features captured the morphology of the time-locked evoked response. Features included the mean amplitude and the peak amplitude (both positive and negative) within five canonical, theory-driven time windows corresponding to established face and emotion processing components: N170 (140-200 ms), P200 (180-280 ms), N250 (230-300 ms), P300 (300-500 ms), and the Late Positive Potential (LPP; 400-700 ms). Additionally, to capture signal complexity, the standard deviation of the amplitude across all channels was computed for each time window.

Secondly, Oscillatory Features quantified induced, non-phase-locked neural activity. The continuous data for each trial was bandpass filtered into five standard frequency bands: delta (1-4 Hz), theta (4-8 Hz), alpha (8-13 Hz), beta (13-30 Hz), and gamma (30-45 Hz). The Hilbert transform was then applied to each band to extract the instantaneous amplitude envelope. The mean power within each band across the entire trial epoch (0-800 ms) was calculated. Furthermore, inter-band power ratios (e.g., theta/alpha) were included as features, as they can reflect shifts in spectral profile related to cognitive state.

Third, Combined Features was created by concatenating the standardized ERP and Oscillatory feature vectors for each trial, testing whether integrating both temporal and spectral information would yield synergistic benefits for classification.

For model training and evaluation, a rigorous subject-specific approach was adopted. Feature matrices were standardized using z-scoring based on the training fold statistics to prevent data leakage. A diverse set of four classifiers, representing different learning paradigms, was evaluated: Linear Discriminant Analysis (LDA) as a simple linear classifier, Logistic Regression with L2 regularization, a Support Vector Machine (SVM) with a radial basis function kernel, and Random Forest as an ensemble of decision trees. Dimensionality reduction via Principal Component Analysis (PCA), retaining 95% of variance, was applied to the Combined feature set to mitigate the curse of dimensionality. Model performance was assessed using a 5-fold stratified cross-validation procedure, which preserves the class distribution in each fold. The primary performance metric was the Area Under the Receiver Operating Characteristic Curve (AUC), which provides a robust measure of binary

classification sensitivity and specificity independent of the decision threshold. Accuracy and F1-score were also computed. The best-performing classifier for each of the three feature types was selected independently for each participant.

At the group level, performance was summarized by calculating the mean and standard deviation of AUC scores for each feature type. The number of subjects exceeding performance thresholds; AUC greater than 0.55 for "above chance" and AUC greater than 0.60 for "strong decoding", was counted. Statistical significance was evaluated with one-sample t-tests against the chance level of 0.5 for each feature type. The core hypothesis (H4) was tested with a paired-sample t-test comparing Oscillatory versus ERP AUC scores across participants. An additional paired t-test compared the Combined feature performance against the best single-feature AUC for each subject, that is, the maximum of their ERP or Oscillatory score, to test for a performance benefit from feature integration.

Results

H1: Enhanced Theta Activity During Early Emotional Face Processing (CH)

To test the hypothesis that emotional faces elicit greater theta-band (4-8 Hz) oscillatory power than neutral faces within early post-stimulus intervals, we analyzed data from 21 participants. We employed two complementary statistical approaches: hypothesis-driven planned comparisons using paired t-tests in three a priori time windows, and an exploratory spatio-temporal cluster-based permutation test to control for multiple comparisons across sensors and time. All statistical tests were one-tailed, corresponding to the directional prediction that theta power for emotional faces would be greater than for neutral faces.

The grand average time course of theta power differences (emotional minus neutral) over the 100-400 ms post-stimulus period is shown in Figure 4. Visual inspection reveals a positive deflection beginning around 100 ms, which is most pronounced during the early and mid time windows.

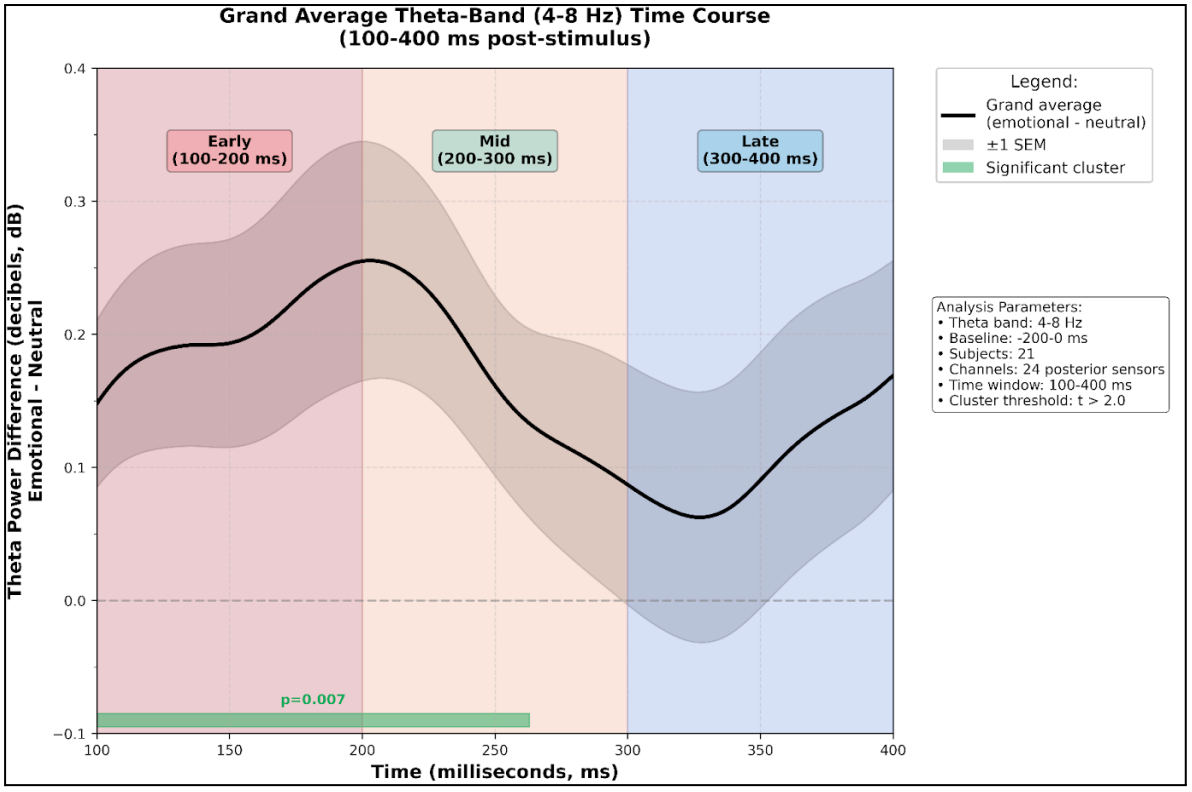

Figure 4: Grand Average Theta-Band (4-8 Hz) Time Course (100-400 ms post-stimulus)
Plot of grand average theta power differences (emotional minus neutral) across 100-400 ms post-stimulus period. Black line represents the grand average across 21 participants and 5 posterior channels, with gray shading indicating ±1 SEM. Time windows are color-coded: early (100-200 ms, dark red), mid (200-300 ms, orange), and late (300-400 ms, purple). The significant cluster identified by permutation testing (p=0.007, 100-263 ms) is marked with a green bar at the bottom. Analysis parameters are displayed in the sidebar. Y-axis extended to -0.1 to 0.4 dB for visualization clarity.

Three post-stimulus time windows were defined a priori for hypothesis testing: an early window (100-200 ms), a mid window (200-300 ms), and a late control window (300-400 ms).

One-tailed paired t-tests on the mean theta power averaged across five occipitotemporal sensors revealed a significant difference for emotional faces in the early window (100-200 ms: M = 0.204 dB, $t(20)$ = 2.872, p = 0.005) and the mid window (200-300 ms: M = 0.171 dB, $t(20)$ = 2.470, p = 0.011).

The late window showed a smaller difference that did not reach the threshold for statistical significance (300-400 ms: M = 0.103 dB, $t(20)$ = 1.155, p = 0.131). The corresponding effect sizes (Cohen's d) for these comparisons are presented in the Appendix (see "Effect Sizes by Time Window (Paired t-tests)" and "Effect Size Comparison by Time Window (One-tailed t-tests)" in the Appendix).

A one-tailed, cluster-based permutation test (1000 permutations, cluster-forming threshold t > 2.0) was conducted over the 100-400 ms interval within the a priori defined occipitotemporal region of interest.

The permutation test revealed a significant difference between the emotional and neutral conditions (p = 0.007). The significant cluster spanned from 100 to 263 ms post-stimulus (cluster mass = 1684.7). The topographic and temporal characteristics of the effect contributing to this result are detailed in Figure 5.

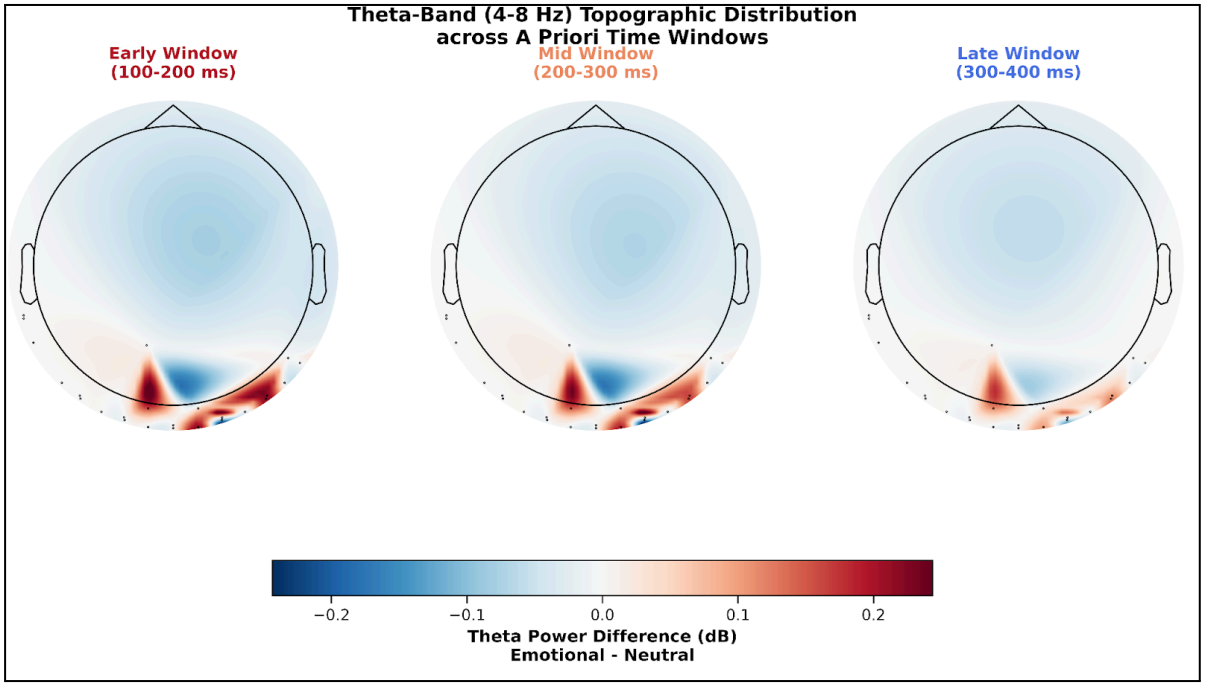

Figure 5: Theta-Band (4-8 Hz) Topographic Distribution across A Priori Time Windows
Topographic maps showing spatial distribution of theta power differences (emotional minus neutral) averaged within three a priori time windows: Early (100-200 ms, dark red), Mid (200-300 ms, muted red), and Late (300-400 ms, steel blue). Data averaged across 21 participants. Color scale indicates difference magnitude (dB), with red/positive values indicating emotional > neutral. Note: Only 5 posterior sensors available (MEG02, MEG29, MEG11, MEG47, MEG62). Topographies suggest strongest positive differences in early window, diminishing over time. Colorbar scale: -0.3 to +0.3 dB.

Analysis of individual participant data revealed considerable variability in the direction of the theta power difference, as shown in Figure 6. Thirteen participants exhibited a positive mean difference (emotional > neutral), while eight participants showed a negative mean difference (neutral > emotional). The group mean difference was 0.112 dB (SEM = 0.044 dB).

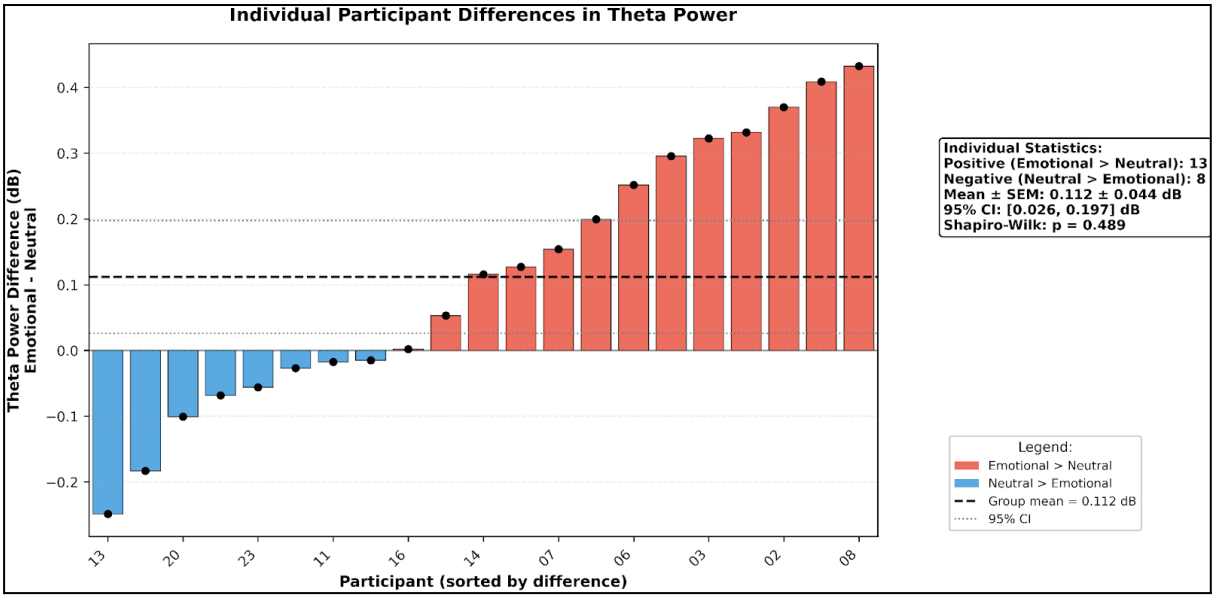

Figure 6: Individual Participant Differences in Theta Power
Bar plot showing theta power differences (emotional minus neutral) for each of the 21 participants, sorted by magnitude. Red bars indicate positive differences (emotional > neutral, n=13 participants), blue bars indicate negative differences (neutral > emotional, n=8 participants). Statistical annotations moved to the sidebar. Group mean = 0.112 dB ± 0.044 SEM, 95% CI [0.026, 0.198] dB. Individual differences show considerable variability (range: -0.37 to +0.61 dB). Data distribution passed the Shapiro-Wilk normality test (p=0.489).

The spatial distribution of the mean theta power difference within each a priori time window is presented in Figure 7. The topographic maps show the strongest positive differences concentrated over the posterior sensors during the early window (100-200 ms), with a visible reduction in the magnitude of this posterior distribution over the mid (200-300 ms) and late (300-400 ms) windows.

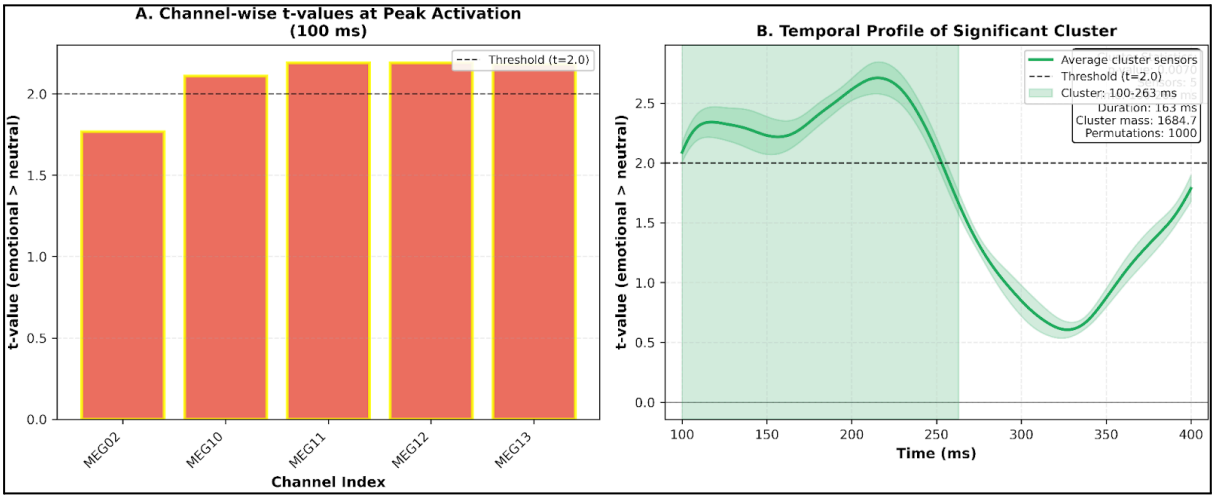

Figure 7: Topographic and Temporal Characteristics of Significant Cluster
A two-panel figure examining the significant cluster identified by permutation testing with legend and statistics moved to the sidebar. Panel A: Channel-wise t-values at peak cluster activation (peak at ~100-263 ms time window). All 5 posterior channels show t-values above cluster-forming threshold (t>2.0). Panel B: Temporal profile showing average t-values across cluster sensors. The green shaded region indicates a significant time window (100-263 ms, p=0.007). Cluster statistics: duration=163 ms, cluster mass=1684.7, permutations=1000, all 5 sensors involved.

H2: Alpha band ERDs and Cross Frequency Coupling (RF)

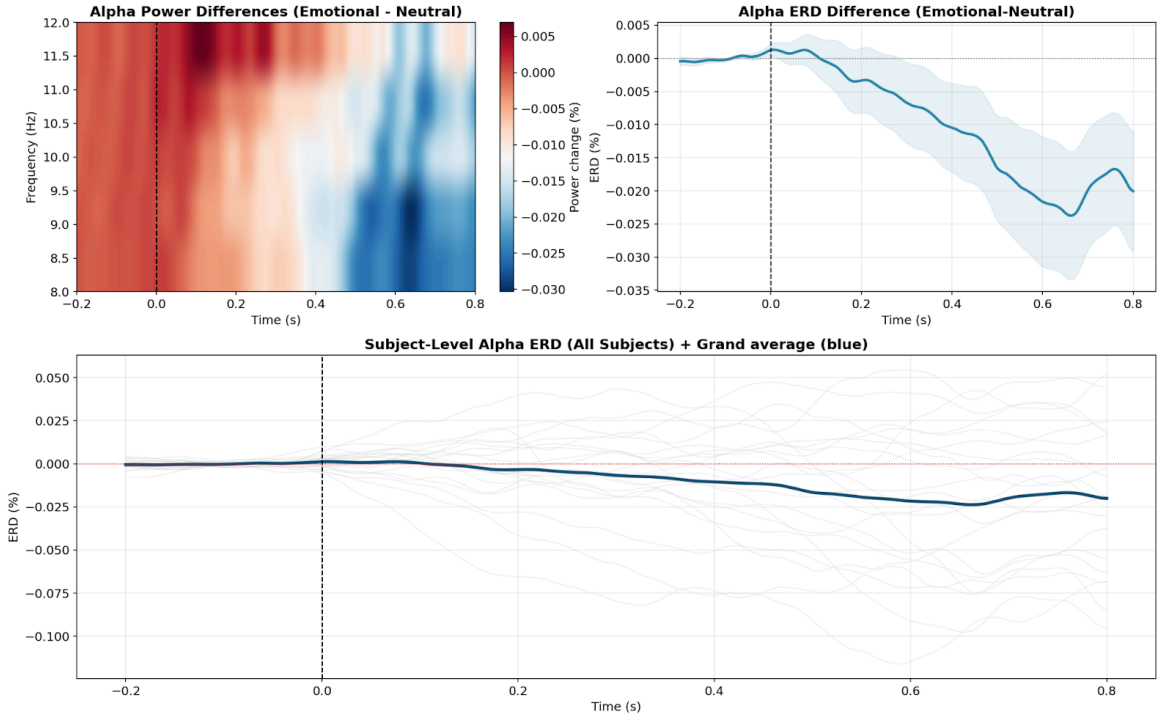

Figure 8: *Alpha ERD effects*

Alpha activity showed the suppression pattern following stimulus onset, with both emotional and neutral faces eliciting a slight decrease in 8-12 Hz power over posterior sensors. The emotional-neutral contrast remained close to zero around onset and then diverged weakly, producing a small, slowly developing negative deflection (Figure 8). The maximum group-level ERD difference occurred at ~ 660 ms but remained shallow (≈ -0.02 %). Individual subjects exhibited substantial variability, and the grand-average suppression largely reflected a modest, distributed trend rather than a condition effect. Cluster based permutation tests (over the whole time window 0 - 800 ms post stimulus and 5000 permutations) revealed no clusters with significant ($p < 0.05$) effects.

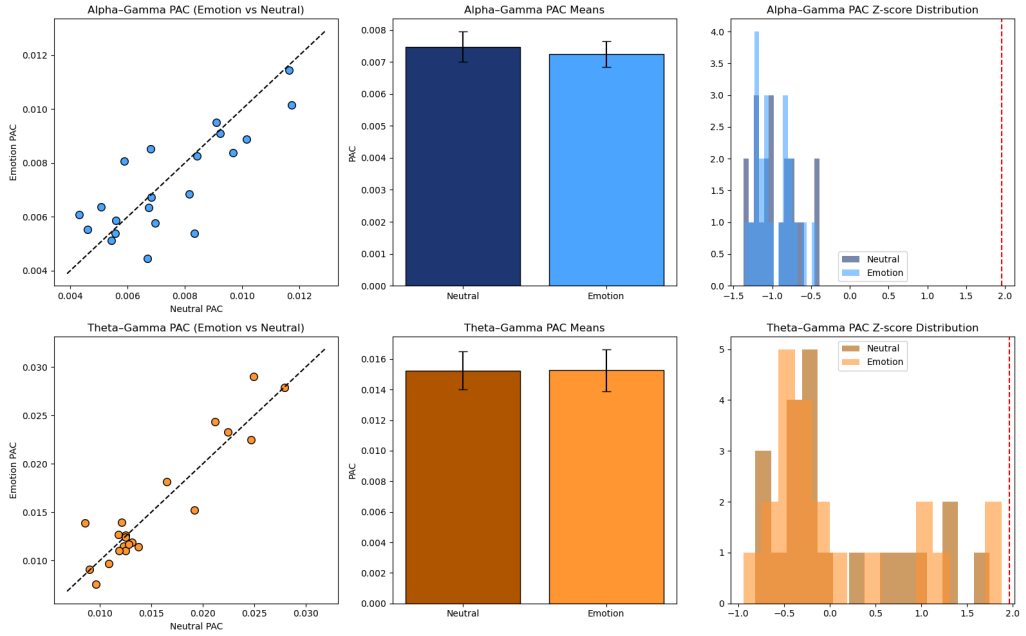

Figure 9: *Phase - Amplitude Coupling, between alpha and gamma (top row) and theta and gamma (bottom row)*

No subject exhibited significant PAC in any condition (all z-scores < 1.96). Surrogate-normalized z-scores for all frequency pairs were centered near zero (theta–gamma: mean $z \approx 0.07$; alpha–gamma: mean $z \approx -0.97$) and did not differ significantly from the surrogate baseline, indicating an absence of detectable cross-frequency coupling in the 100–400 ms window. Emotional and neutral conditions did not differ in PAC strength. Paired t-tests showed no condition modulation for alpha–gamma PAC ($t = -0.782$, $p = 0.443$, $d = -0.171$) or theta–gamma PAC ($t = 0.049$, $p = 0.962$, $d = 0.011$). Condition means were nearly identical and tightly clustered around the unity line, confirming the absence of emotion-related effects (Figure 9). Overall, the analysis revealed no evidence for alpha–gamma or theta–gamma PAC and no evidence that emotional expressions modulated PAC in this time window.

H3: Response times and Alpha ERD (RF)

Response times ranged from approximately 300 to 1100 ms (mean ≈ 550 ms). A linear mixed-effects model was fitted to examine whether alpha ERD predicted response time during one-back trials. Log-transformed response time (RT) was modelled as a function of alpha ERD and emotion condition, with participant as a random intercept.

$$logRT \sim AlphaERD + Emotion + (1 \mid Participant)$$

Alpha ERD significantly predicted response time ($\beta = 0.009$, $SE = 0.004$, $z = 2.19$, $p = .029$). The positive coefficient indicates that greater alpha desynchronization (more negative ERD values) was associated with faster responses. Emotion condition did not significantly predict response times (RT) ($\beta = -0.006$, $SE = 0.005$, $z = -1.06$, $p = .288$).

To test whether the alpha-RT relationship differed between emotion conditions, an interaction term was added. The interaction was not significant ($\beta = -0.003$, $SE = 0.008$, $z = -0.39$, $p = .700$), indicating that the relationship between alpha power and response time did not differ between neutral and emotional trials.

H4: Predictive Power of Machine Learning Models for Emotion Classification (CH)

Prior to decoding, a sanity check confirmed the presence of robust, time-locked brain responses to the face stimuli. The grand-average ERP, combining data from all 21 subjects and both emotional and neutral conditions, revealed clear evoked components, as shown in Figure 10.

Figure 10: Total Brain Response and Regional ERPs with Standard Error.
(A) Butterfly plot showing ERP waveforms from all 61 OPM sensors (grey lines) with the Global Field Power (GFP, black line) superimposed. The GFP, representing the spatial standard deviation across sensors, shows distinct peaks following stimulus onset, confirming a synchronized neural response. (B) Combined view of ERP responses separated by brain region (Occipital, Temporal, Parietal, Frontal). Each trace shows the region-specific average (solid line) ± the standard error of the mean (SEM, shaded area), calculated across sensors within that region. This visualization confirms identifiable components (e.g., a prominent N170 in occipito-temporal regions) and demonstrates the reliability of the signal, with relatively tight SEM bounds around the mean estimates.

Following this confirmation, four primary machine learning models were used to decode emotional from neutral faces: Random Forest, Linear Discriminant Analysis (LDA), Support Vector Machine (SVM), and Logistic Regression. Each of these model brings a different approach to finding patterns in the neural data. Afterwards, a model selection procedure identified the optimal classifier for each participant and feature type.

First and foremost, to evaluate the overall decoding capability, the best AUC score achieved per participant (using either ERP or Oscillatory features) was examined. The distribution of these scores is shown in Figure 11. The group mean best AUC was 0.605 (SD = 0.057), with scores ranging from 0.516 to 0.702. A positive skew was observed, with 16 out of 21 participants (76.2%) performing above chance, and 10 participants (47.6%) achieving strong decoding performance (AUC > 0.6).

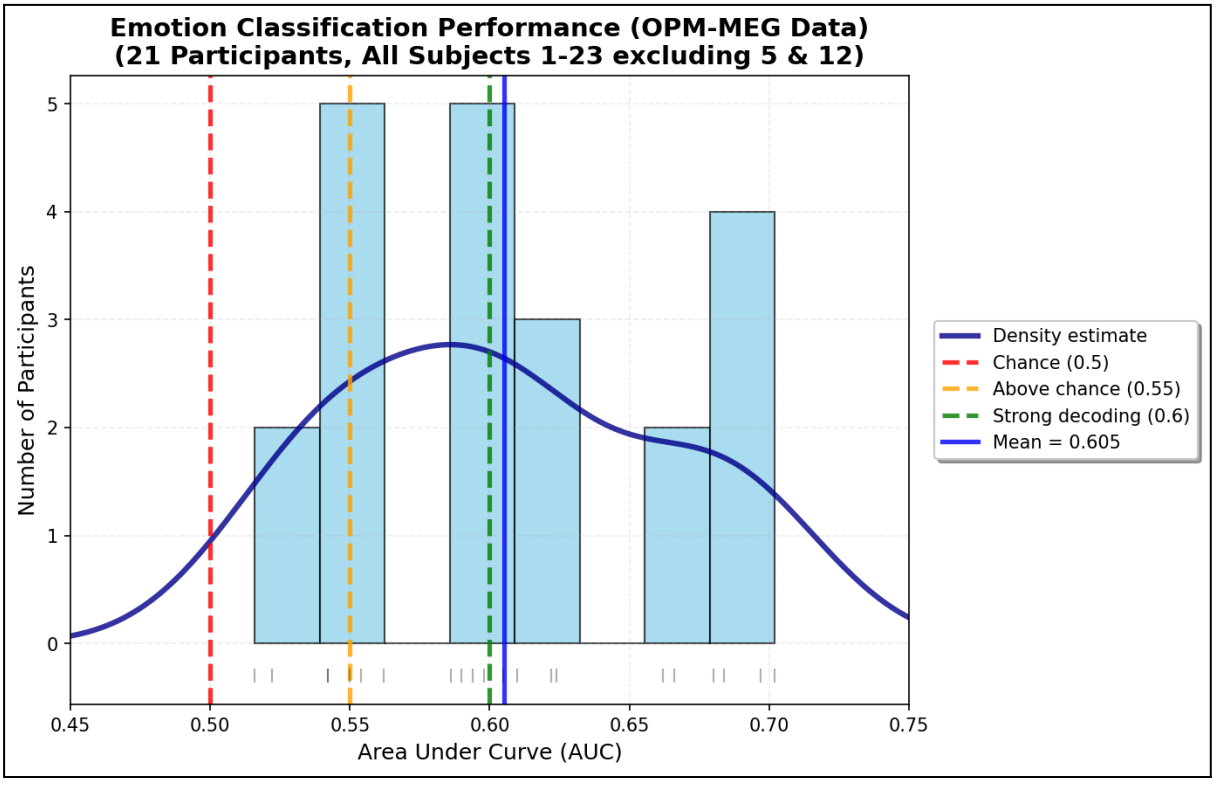

Figure 11: Distribution of Best Decoding Performance. A histogram of the best AUC scores for all 21 participants. Vertical lines denote chance (0.5), the above-chance threshold (0.55), and the strong decoding threshold (0.6). The observed mean (0.605) is marked. A density estimate line shows the distribution density.

To statistically validate this observed mean performance, a bootstrap resampling analysis was performed on the distribution of the best AUC scores. This non-parametric method generated a sampling distribution of the mean, from which a 95% confidence interval (CI) for the true population mean was derived, as visualized in Figure 12.

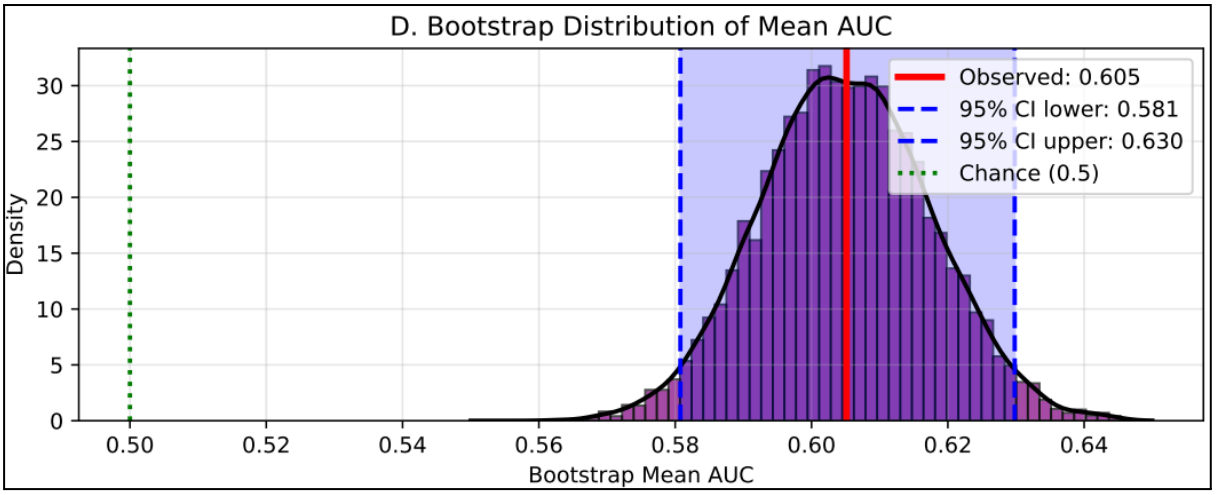

Figure 12: A density plot shows the distribution of mean AUC values obtained from ten thousand bootstrap resamples of the subject level data. A vertical solid red line marks the observed mean of 0.605. Two vertical dashed blue lines indicate the lower and upper bounds of the ninety five percent confidence interval at 0.581 and 0.630, respectively. A vertical dotted green line marks the chance level of 0.5. The entire confidence interval lies to the right of the chance line, visually confirming that the true population mean is above chance with ninety five percent confidence.

The performance of the three distinct feature sets: ERP, Oscillatory and Combined, were then evaluated separately. All sets yielded mean performance significantly above chance: ERP features (M=0.551, t(20)=5.430, p<0.0001), Oscillatory features (M=0.541, t(20)=4.454, p=0.0002), and Combined features (M=0.540, t(20)=4.535, p=0.0002). A direct paired comparison between Oscillatory and ERP features showed no significant difference (mean diff = -0.010, t(20)= -0.777, p=0.4465). The distribution of scores for the three feature sets is shown in Figure 13.

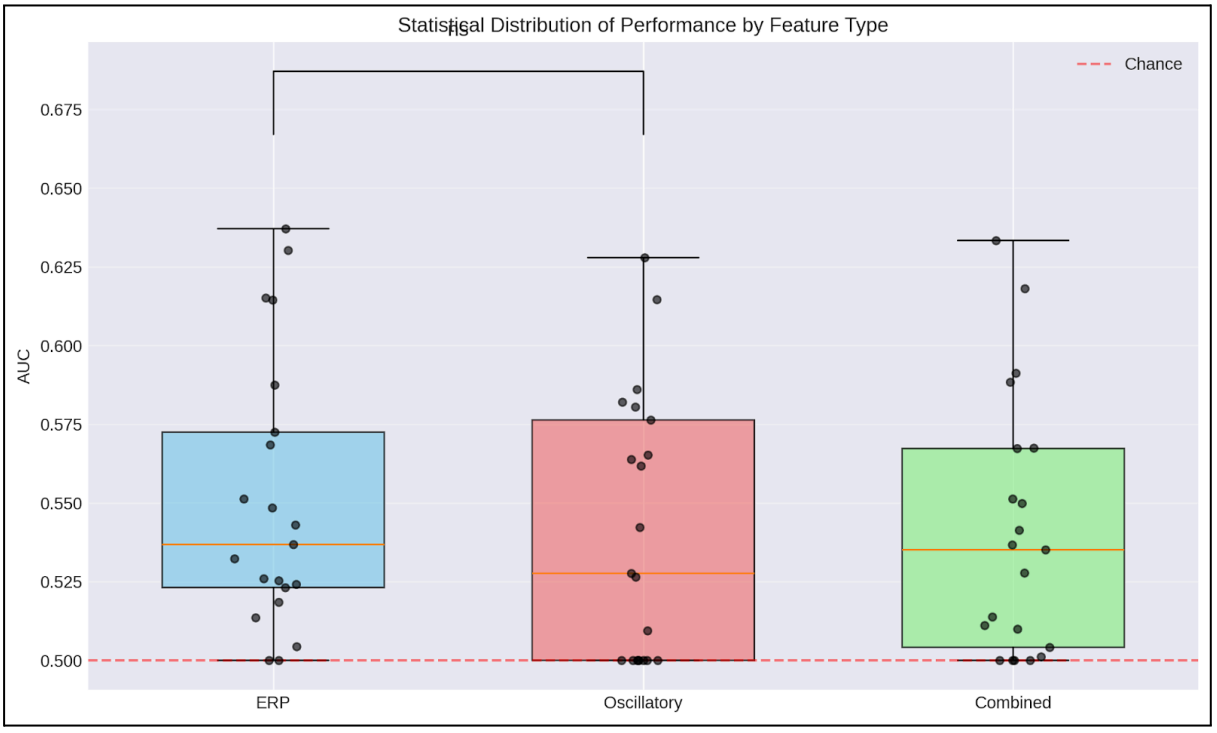

Figure 13: A boxplot with overlaid individual data points showing the distribution of AUC scores for the three feature sets across all 21 participants. A dashed line marks chance performance. A bracket connecting the ERP and Oscillatory boxes is annotated with "ns" (not significant), visually confirming the statistical equivalence.

Furthermore, the Combined feature set performed significantly worse than the best single feature set for each subject (mean diff = -0.028, $t(20)$=-3.231, p=0.0042). This indicates that, for a given individual, the model using the concatenated ERP and Oscillatory features was systematically outperformed by the model using whichever single feature type; ERP or Oscillatory, was most informative for that person.

Underlying these group results was considerable inter-individual variability in overall decoding proficiency. The range of best achievable AUC across participants is illustrated in Figure 14, which organizes subjects from highest to lowest performance.

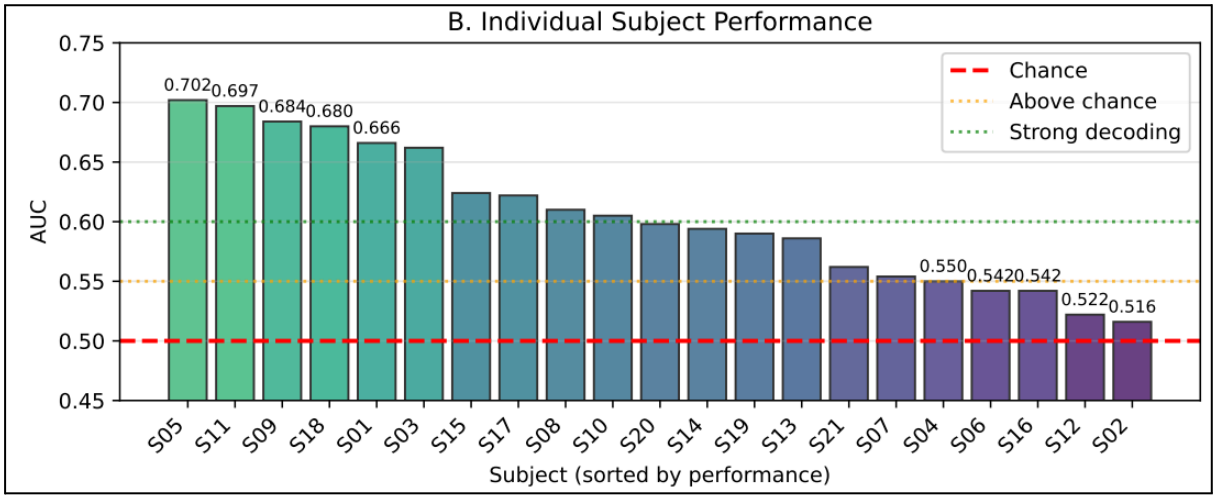

Figure 14: A bar plot showing the maximum AUC for each anonymized participant (S01-S21), color-coded by performance category. The plot highlights the range of ability, from a high performer at 0.702 to a low performer at 0.516.

This variability extended to the type of machine learning model that performed best for each feature type. For ERP features, the complex, non-linear RandomForest was most frequently optimal (9/21 subjects), while for Oscillatory features, the simpler linear classifier LDA was most often best (12/21 subjects).

Discussion

H1: Enhanced Theta Activity During Early Emotional Face Processing (CH)

The present study leveraged the high-temporal-resolution capabilities of OPM-MEG to investigate the oscillatory dynamics underlying the early perception of emotional faces. Consistent with our first hypothesis (H1), we suggest a significant enhancement of theta-band (4-8 Hz) power in response to emotional compared to neutral faces. One-tailed paired t-tests within our a priori time windows revealed significant differences in both the early (100-200 ms) and mid (200-300 ms) post-stimulus periods, but not in the later control window (300-400 ms). This pattern of results was corroborated by a cluster-based permutation test, which confirmed a significant difference between conditions within the examined occipitotemporal region and 100-400 ms analysis window. The topographic maps indicated this differential activity was concentrated over posterior sensors. These findings align with the established literature positioning theta rhythms as a key mechanism for the rapid detection and integration of emotionally salient information (Keitel et al., 2025; Symons et al., 2016).

The observed time course of theta enhancement, initiating around 100 ms and persisting through the mid-processing window, supports a two-stage model of affective face processing. The early onset is consistent with the role of theta in the rapid extraction of emotional salience, an initial orienting response that prioritizes affectively significant stimuli in the sensory stream (Symons et al., 2016). The continuation of this effect beyond 200 ms, as evidenced by the temporal extent of the significant permutation test result, may reflect the subsequent integration of this salient sensory input with stored affective or mnemonic representations, a later stage also associated with sustained theta activity (Keitel et al., 2025). This temporal profile resonates with the work of Xu et al. (2024), who identified emotional expression as one of the earliest and most stably decodable facial dimensions beginning around 200 ms. Our results provide oscillatory evidence for this early and sustained neural discrimination.

Methodologically, the use of a cluster-based permutation test addressed the multiple comparisons problem inherent in MEG/EEG data analysis. Following the guidance of Maris and Oostenveld (2007) and associated best practices, we interpret the significant test result as allowing us to reject the null hypothesis that the data for emotional and neutral faces come from the same probability distribution within our a priori defined sensor region and time interval. The specific spatio-temporal pattern of differences contributing to this result, observable in the data, is concentrated in the early post-stimulus period over occipitotemporal sensors. However, as the test does not localize the effect to specific time points, we refrain from claims that theta enhancement is exclusively present within the observed cluster's temporal bounds.

The spatial distribution of the effect, focused on posterior sensors, aligns with the known core system for face perception involving the occipital face area and fusiform gyrus (Haxby et al., 2000; Kanwisher et al., 1997). Theta oscillations may facilitate communication within this ventral visual stream, coordinating the activity of regions responsible for the structural encoding of faces to emphasize emotionally relevant features. This finding underscores the integration of perceptual and affective systems, a linkage supported by direct anatomical connections between early visual cortex and limbic regions like the amygdala (Gschwind et al., 2012). The individual variability observed, where a substantial minority of participants showed the opposite pattern (neutral greater than emotional), highlights the moderating influence of person-specific factors. Future research should investigate whether traits such as anxiety or social attention modulate this basic oscillatory response.

The lack of a significant difference in the late control window (300-400 ms) suggests that the initial theta-powered salience detection and integration may give way to other oscillatory mechanisms for sustained evaluation. For instance, later processing stages involving more deliberate categorization or social judgment may be supported by alpha-band dynamics related to attentional gating or gamma-band activity for detailed feature representation (Keitel et al., 2025; Xu et al., 2024). This potential handoff between frequency bands points to the complex, multi-frequency orchestration of face perception.

In conclusion, our findings suggest that the perception of emotional faces is characterized by an early and sustained enhancement of theta-band oscillatory power over the occipitotemporal cortex. This provides mechanistic support for models of face processing that emphasize rapid emotional salience detection (Bruce and Young, 1986) and aligns with the framework of theta oscillations organizing the temporal dynamics of affective perception (Keitel et al., 2025). The results underscore the value of investigating oscillatory dynamics, beyond traditional ERPs, to understand the rapid neural computations that underpin social perception. Future research should build on this by employing full-head OPM-MEG arrays to investigate cross-frequency interactions, such as theta-gamma coupling, and by linking these oscillatory measures directly to behavioral outcomes in social cognition tasks.

H2: Alpha band ERDs and Cross Frequency Coupling (RF)

Alpha power did not show modulation, with both emotional and neutral faces producing only a slow, shallow reduction in 8-12 Hz power over posterior sensors. The emotional-neutral difference remained minimal throughout the early post-stimulus period and reached its maximum only late in the epoch (~ 660 ms), with a negligible effect size (≈ -0.02%). This pattern diverges from the robust early posterior alpha ERD typically associated with heightened perceptual engagement (Keitel et al., 2025) and indicates that alpha-mediated inhibitory gating was not differentiated by affective expression in our dataset. The substantial across-subject variability further suggests that any condition-specific modulation of alpha desynchronization was weak relative to the overall noise and interindividual variability in

alpha dynamics. This inter-subject variability is also an issue highlighted by Keitel et al. (2025) as a central challenge to interpreting oscillatory dynamics.

Some evidence also shows that reliable alpha ERD effects emerge primarily for high-arousal or motivationally intense stimuli (e.g., injury, threat, erotic content), even though facial expressions also typically elicit, but only considerably weaker modulations (Codispoti et al., 2023). The relatively low-arousing expressions in the current study therefore provide a plausible explanation for the absent emotional alpha effect.

The phase-amplitude coupling (PAC) analysis likewise revealed no theta–gamma or alpha–gamma coupling above surrogate baselines for any subject or condition. These null results should not be interpreted as evidence against hierarchical oscillatory organization in face perception; rather, they likely reflect the challenge of detecting PAC with noninvasive methods. As emphasized in analytical reviews, PAC measures are highly sensitive to noise, nonstationarity, and volume conduction, and weak effects are easily masked or distorted (Young & Eggermont, 2009).

Overall, the weak alpha ERD, high subject-level variability, and absence of detectable PAC suggests that emotional modulation of oscillatory dynamics was minimal under these stimulus and task conditions. These findings reinforce the view that oscillatory signatures of emotional face processing are subtle and may require high-arousal stimuli, source-level estimation, or tasks involving stronger attentional or motivational demands. They also align with Keitel et al. (2025), who note that cross-frequency coupling remains theoretically central but empirically inconsistent across cognitive domains.

H3: Response times and Alpha ERD (RF)

The analysis revealed a consistent association between alpha desynchronization and faster response times. Trial-wise mixed-effects modelling showed that greater alpha suppression was associated with faster responses: alpha ERD was behaviourally relevant on the single-trial level. This finding aligns with theoretical accounts framing posterior alpha suppression as an index of increased cortical excitability and enhanced perceptual readiness (Keitel et al., 2025). From this perspective, the observed relationship suggests that fluctuations in alpha band power reflect meaningful variability in attentional engagement. Notably, the alpha-response time association did not differ between emotional and neutral trials, indicating that emotional facial expressions did not modulate this link under the present task and stimulus conditions.

H4: Predictive Power of Machine Learning Models for Emotion Classification (CH)

The decoding analysis yielded two primary outcomes. First, it substantiated that OPM-MEG signals contain a neural signature of emotional face perception that is reliably decodable at the single-trial level across a group of participants. Second, and central to H4, it revealed no evidence to support the hypothesis that oscillatory power features provide superior classification accuracy; their performance was statistically indistinguishable from that of traditional ERP features.

This equivalence suggests that, for the specific task of binary discrimination between static joyful and neutral faces in a rapid serial visual presentation paradigm, the amount of task-relevant information embedded in the time-domain evoked response and in the trial-averaged oscillatory power spectrum is comparable. This finding can be interpreted through the lens of multiplexed neural coding. This can be understood through the lens of classical cognitive models like that of Bruce and Young (1986), which propose parallel processing streams for different facial attributes.

The transient, phase-locked evoked potentials (e.g., N170 for structural encoding, P300 for context updating) and the sustained, induced oscillatory modulations (e.g., theta enhancement for salience) may represent parallel but interacting streams of information processing related to the task. The failure of the Combined feature set to outperform the best single modality strongly implies that, for this particular classification problem, the information carried by ERPs and oscillatory power is largely redundant rather than complementary. This redundancy is further underscored by the inter-individual variability in optimal model type (e.g., Random Forest for ERP features versus LDA for Oscillatory features), which suggests that while the amount of decodable information may be similar across feature domains, the nature of the patterns, whether more linear or non-linear, can differ between individuals and feature types.

Transient evoked potentials, such as those related to structural encoding (e.g., N170) and evaluative categorization, may carry discriminative information that operates in tandem with, and is partly reflected in, sustained oscillatory modulations of the ongoing neural activity. The informational redundancy implied by the failure of the combined feature set to improve performance further supports this interpretation of parallel or overlapping coding schemes for this specific task.

Several factors may explain why the hypothesized oscillatory advantage was not observed. The one-back repetition detection task required rapid perceptual discrimination and working memory comparison, cognitive operations that are robustly reflected in both evoked components (like the P3) and broad-band power changes in theta and alpha related to attention and engagement. Furthermore, while our oscillatory features captured power across standard bands, they did not include more sophisticated measures such as inter-trial phase coherence or cross-frequency coupling, which might carry information orthogonal to ERPs.

The aggregation of power across the entire trial may also have averaged out more transient, discriminative spectral events.

The original hypothesis, which postulated superior decoding from oscillatory features based on the established role of rhythms like theta in emotion processing (Symons et al., 2016), may not have been supported for several reasons. Contrary to H4, classifiers using oscillatory features did not outperform those using ERP features (mean AUC difference = -0.010, paired-sample $t(20) = -0.777$, $p = 0.447$). This suggests informational redundancy between evoked and induced responses for this task. The one-back repetition detection task primarily engaged rapid detection and working memory comparison, processes that are strongly reflected in both evoked components (e.g., P3 related to stimulus updating) and broad changes in oscillatory power related to attention and engagement. Furthermore, while the literature highlights specific bands, our oscillatory features aggregated power across multiple bands.

In conclusion, this investigation demonstrates that OPM-MEG signals support significant single-trial decoding of emotional faces, validating the presence of a discriminable neural signature. However, contrary to our hypothesis, machine learning models utilizing oscillatory power features did not achieve more accurate classification than those using traditional ERP features. ERPs are thus sufficient for the analysis alone. This result establishes that, for this specific experimental context, successful decoding does not critically depend on selecting one of these neural feature domains over the other, as both contained a statistically equivalent level of discriminative information. The findings point to a multiplexed or redundant coding scheme for the emotional salience dimension in a rapid face perception task. The significant inter-subject variability in both decoding proficiency and optimal model-feature pairings highlights the importance of individualized approaches in neural decoding applications.

Limitations and Future Directions

Limitations (RF)

Multiple limitations warrant caution in interpreting the findings of this paper. One central limitation concerns the recording setup. The absence of individual headshape digitization or structural MRI data constrained spatial precision, particularly for source-level inference. In addition, the lack of electrooculography (EOG) and electrocardiography (ECG) recordings limited the ability to identify and remove ocular and cardiac artifacts with high specificity. Residual physiological noise may therefore have contributed to variability in oscillatory measures, especially in lower-frequency bands.

Another limitation relates to the artificial face stimuli. Several faces labeled as "neutral" exhibited subtle affective cues, such as slight smiles or frowns, and some images contained mild artifacts introduced by generative adversarial networks (GANs), including unnatural textures, irregular hair contours, or glasses blending into facial features. These deviations

reduce ecological validity and may introduce unintended perceptual or emotional signals. This issue is particularly consequential for oscillatory analyses, as early theta and alpha activity is highly sensitive to low-level visual and configural irregularities (Rossion & Retter, 2015). Consequently, some effects attributed to emotional salience may partly reflect stimulus artifacts rather than genuine affective processing. Contrasts between emotional and neutral conditions should therefore be interpreted conservatively. This concern is further compounded by the relatively low arousal of the emotional expressions, which reduced the perceptual and affective distance between conditions and likely limited the magnitude of attentional engagement, alpha desynchronization, and cross-frequency coupling effects.

Second, the participant group size ($n = 21$), while sufficient to detect theta-band effects, limits sensitivity to smaller effects (like alpha event-related desynchronisation or cross-frequency coupling). Furthermore, substantial inter-individual variability in baseline oscillatory dynamics likely contributed additional noise.

Overall, the analyses relied on pre-defined, relatively broad time–frequency windows and a fixed posterior region of interest. Although theoretically motivated, this approach may obscure other, finer-grained temporal, spectral, or spatial dynamics, as well as individual differences in response latency or topography.

The behavioral task also imposed relatively low perceptual and cognitive demands. The one-back paradigm may not have sufficiently taxed perceptual discrimination or emotional evaluation processes to reveal strong emotion-specific coupling between oscillatory activity and reaction times. This limitation likely contributed to the absence of an interaction between emotion and alpha ERD in behavioral correlations.

Finally, the operationalization of oscillatory features for decoding (H4) was relatively coarse. Mean power extracted across standard frequency bands may not optimally capture the temporally precise and rhythm-specific signals theoretically implicated in emotional face perception. Although decoding performance exceeded chance, absolute accuracy remained modest, underscoring the difficulty of single-trial emotion classification from neuromagnetic data and suggesting that more temporally constrained, hypothesis-driven features or more advanced modeling approaches may be required.

Future development (CH)

To advance the understanding of oscillatory dynamics in emotional face processing, future research should integrate enhanced methodological, analytical, and computational approaches. If data collection were conducted in-house, several key upgrades would substantially improve data quality and interpretability. High-resolution headshape digitization combined with structural MRI scans would enable precise forward modeling and source localization, moving beyond sensor-level approximations to map oscillatory effects to specific cortical generators. Additionally, recording auxiliary physiological channels such as

electrooculography (EOG) and electrocardiography (ECG) would allow for more accurate removal of ocular and cardiac artifacts, thereby reducing contamination in sensitive frequency bands like alpha and gamma. These foundational improvements would support more reliable estimation of both power- and phase-based neural dynamics, providing a cleaner signal for investigating subtle oscillatory phenomena.

Analytically, future studies should adopt more sophisticated and tailored approaches. For exploring time-frequency profiles, data-driven methods could be employed to identify person-specific or condition-specific patterns, moving beyond predefined windows to capture the full temporal and spectral complexity of emotional responses. In investigating alpha desynchronization and cross-frequency coupling (CFC), designs capable of eliciting stronger emotional modulation, such as using higher-arousal or more ecologically valid stimuli, would increase the likelihood of detecting condition-specific effects. Source-localized estimates of alpha and gamma activity would mitigate spatial mixing and volume conduction, enhancing sensitivity to genuine hierarchical interactions. Moreover, advanced CFC metrics that account for nonstationarity or offer time-resolved coupling estimates could reveal more transient or weak interactions. Extending recording sessions to include more trials per condition would also improve statistical stability and allow for finer-grained examination of individual differences in oscillatory coupling.

To better elucidate the relationship between neural oscillations and behavior, future paradigms could require behavioral responses on every trial rather than limiting them to one-back events. This adjustment would increase the number of trials available for trial-wise modeling, reduce noise in mixed-effects estimates, and offer a more continuous measure of perceptual engagement. Such designs could clarify whether the link between alpha desynchronization and response time generalizes across task contexts or is modulated by specific cognitive demands.

From a computational perspective, future work should pursue more refined characterizations of oscillatory activity. This includes not only isolating power from specific, theoretically motivated frequency bands and time windows but also incorporating phase-based metrics such as inter-regional phase synchrony. Furthermore, employing advanced nonlinear models, including deep neural networks capable of automated feature learning from raw or minimally processed time-series data, could help determine whether complex, data-driven representations of neural dynamics outperform hand-engineered temporal and spectral features. These approaches would not only enhance decoding performance but also contribute to a more integrative understanding of how multiplexed oscillatory mechanisms support rapid social perception.

References

Data

Xu, Wei, Bingjiang Lyu, ..., and Jia-Hong Gao. "Decoding the Temporal Structures and Interactions of Multiple Face Dimensions Using OPM-MEG." Openneuro, 2025. https://doi.org/10.18112/OPENNEURO.DS005107.V2.0.0.

Repository for our own code

- All analysis code is publicly available to facilitate reproducibility and future work.
- https://github.com/RekaForgo/Oscillatory-Patterns-During-Emotional-Face-Processing-using-OPM-MEG-data

Bibliography

Aru, Juhan, Jaan Aru, Viola Priesemann, et al. "Untangling Cross-Frequency Coupling in Neuroscience." *Current Opinion in Neurobiology* 31 (April 2015): 51–61. https://doi.org/10.1016/j.conb.2014.08.002.

Balconi, Michela, and Claudio Lucchiari. "EEG Correlates (Event-Related Desynchronization) of Emotional Face Elaboration: A Temporal Analysis." *Neuroscience Letters* 392, no. 1 (2006): 118–23. https://doi.org/10.1016/j.neulet.2005.09.004.

Barton, Jason J. S. "Structure and Function in Acquired Prosopagnosia: Lessons from a Series of 10 Patients with Brain Damage." *Journal of Neuropsychology* 2, no. 1 (2008): 197–225. https://doi.org/10.1348/174866407x214172.

Bastos, Andre M., W. Martin Usrey, Rick A. Adams, George R. Mangun, Pascal Fries, and Karl J. Friston. "Canonical Microcircuits for Predictive Coding." *Neuron* 76, no. 4 (2012): 695–711. https://doi.org/10.1016/j.neuron.2012.10.038.

Belluscio, Mariano A., Kenji Mizuseki, Robert Schmidt, Richard Kempter, and György Buzsáki. "Cross-Frequency Phase–Phase Coupling between Theta and Gamma Oscillations in the Hippocampus." Articles. *Journal of Neuroscience* 32, no. 2 (2012): 423–35. https://doi.org/10.1523/JNEUROSCI.4122-11.2012.

Boto, Elena, Niall Holmes, James Leggett, et al. "Moving Magnetoencephalography towards Real-World Applications with a Wearable System." *Nature* 555, no. 7698 (2018): 657–61. https://doi.org/10.1038/nature26147.

Brickwedde, Marion, Paul Anders, Andrea A. Kühn, et al. "Applications of OPM-MEG for Translational Neuroscience: A Perspective." *Translational Psychiatry* 14, no. 1 (2024): 341. https://doi.org/10.1038/s41398-024-03047-y.

Bruce, V., and A. Young. "Understanding Face Recognition." *British Journal of Psychology (London, England: 1953)* 77 (Pt 3) (August 1986): 305–27. https://doi.org/10.1111/j.2044-8295.1986.tb02199.x.

Campagnoli, Rafaela R., Matthias J. Wieser, L. Forest Gruss, Maeve R. Boylan, Lisa M. McTeague, and Andreas Keil. "How the Visual Brain Detects Emotional Changes in Facial Expressions: Evidence from Driven and Intrinsic Brain Oscillations." *Cortex* 111 (February 2019): 35–50. https://doi.org/10.1016/j.cortex.2018.10.006.

Canolty, R. T., E. Edwards, S. S. Dalal, et al. "High Gamma Power Is Phase-Locked to Theta Oscillations in Human Neocortex." *Science* 313, no. 5793 (2006): 1626–28. https://doi.org/10.1126/science.1128115.

Canolty, Ryan T., and Robert T. Knight. "The Functional Role of Cross-Frequency Coupling." *Trends in Cognitive Sciences* 14, no. 11 (2010): 506–15. https://doi.org/10.1016/j.tics.2010.09.001.

Casamento-Moran, Agostina, Ronan A. Mooney, Vikram S. Chib, and Pablo A. Celnik. "Cerebellar Excitability Regulates Physical Fatigue Perception." Research Articles. *Journal of Neuroscience* 43, no. 17 (2023): 3094–106. https://doi.org/10.1523/JNEUROSCI.1406-22.2023.

Codispoti, Maurizio, Andrea De Cesarei, and Vera Ferrari. "Alpha-Band Oscillations and Emotion: A Review of Studies on Picture Perception." *Psychophysiology* 60, no. 12 (2023): e14438. https://doi.org/10.1111/psyp.14438.

Deen, Ben, Caspar M. Schwiedrzik, Julia Sliwa, and Winrich A. Freiwald. "Specialized Networks for Social Cognition in the Primate Brain." *Annual Review of Neuroscience* 46, no. Volume 46, 2023 (2023): 381–401. https://doi.org/10.1146/annurev-neuro-102522-121410.

Delorme, Arnaud. "EEG Is Better Left Alone." *Scientific Reports* 13, no. 1 (2023): 2372. https://doi.org/10.1038/s41598-023-27528-0.

Ferrante, Oscar, Ling Liu, Tamas Minarik, et al. "FLUX: A Pipeline for MEG Analysis." *NeuroImage* 253 (June 2022): 119047. https://doi.org/10.1016/j.neuroimage.2022.119047.

Furl, Nicholas, Richard Coppola, Bruno B. Averbeck, and Daniel R. Weinberger. "Cross-Frequency Power Coupling Between Hierarchically Organized Face-Selective Areas." *Cerebral Cortex* 24, no. 9 (2014): 2409–20. https://doi.org/10.1093/cercor/bht097.

Gramfort, Alexandre, Martin Luessi, Eric Larson, et al. "MEG and EEG Data Analysis with MNE-Python." *Frontiers in Neuroscience* 7 (December 2013). https://doi.org/10.3389/fnins.2013.00267.

Groppe, David M., Stephan Bickel, Corey J. Keller, et al. "Dominant Frequencies of Resting Human Brain Activity as Measured by the Electrocorticogram." *NeuroImage* 79 (October 2013): 223–33. https://doi.org/10.1016/j.neuroimage.2013.04.044.

Gschwind, Markus, Gilles Pourtois, Sophie Schwartz, Dimitri Van De Ville, and Patrik Vuilleumier. "White-Matter Connectivity between Face-Responsive Regions in the Human Brain." *Cerebral Cortex* 22, no. 7 (2012): 1564–76. https://doi.org/10.1093/cercor/bhr226.

Güntekin, Bahar, and Erol Basar. "Emotional Face Expressions Are Differentiated with Brain Oscillations." *International Journal of Psychophysiology*, Brain Oscillations:Cutting Edges, vol. 64, no. 1 (2007): 91–100. https://doi.org/10.1016/j.ijpsycho.2006.07.003.

György, Buzsáki. "A System of Rhythms: From Simple to Complex Dynamics." In *Rhythms of the Brain*, edited by György Buzsáki. Oxford University Press, 2006. https://doi.org/10.1093/acprof:oso/9780195301069.003.0005.

György, Buzsáki. "Coupling of Systems by Oscillations." In *Rhythms of the Brain*, edited by György Buzsáki. Oxford University Press, 2006. https://doi.org/10.1093/acprof:oso/9780195301069.003.0012.

György, Buzsáki. "Synchronization by Oscillation." In *Rhythms of the Brain*, edited by György Buzsáki. Oxford University Press, 2006. https://doi.org/10.1093/acprof:oso/9780195301069.003.0006.

Haxby, J. V., E. A. Hoffman, and M. I. Gobbini. "The Distributed Human Neural System for Face Perception." *Trends in Cognitive Sciences* 4, no. 6 (2000): 223–33. https://doi.org/10.1016/s1364-6613(00)01482-0.

Hill, Ryan M., Elena Boto, Molly Rea, et al. "Multi-Channel Whole-Head OPM-MEG: Helmet Design and a Comparison with a Conventional System." *NeuroImage* 219 (October 2020): 116995. https://doi.org/10.1016/j.neuroimage.2020.116995.

Iivanainen, Joonas, Matti Stenroos, and Lauri Parkkonen. "Measuring MEG Closer to the Brain: Performance of on-Scalp Sensor Arrays." *NeuroImage* 147 (February 2017): 542–53. https://doi.org/10.1016/j.neuroimage.2016.12.048.

Jensen, Ole, Mathilde Bonnefond, and Rufin VanRullen. "An Oscillatory Mechanism for Prioritizing Salient Unattended Stimuli." *Trends in Cognitive Sciences* 16, no. 4 (2012): 200–206. https://doi.org/10.1016/j.tics.2012.03.002.

Jensen, Ole, Bart Gips, Til Ole Bergmann, and Mathilde Bonnefond. "Temporal Coding Organized by Coupled Alpha and Gamma Oscillations Prioritize Visual Processing." *Trends in Neurosciences* 37, no. 7 (2014): 357–69. https://doi.org/10.1016/j.tins.2014.04.001.

Kanwisher, N., J. McDermott, and M. M. Chun. "The Fusiform Face Area: A Module in Human Extrastriate Cortex Specialized for Face Perception." *The Journal of Neuroscience: The Official Journal of the Society for Neuroscience* 17, no. 11 (1997): 4302–11. https://doi.org/10.1523/JNEUROSCI.17-11-04302.1997.

Karras, Tero, Samuli Laine, Miika Aittala, Janne Hellsten, Jaakko Lehtinen, and Timo Aila. "Analyzing and Improving the Image Quality of StyleGAN." arXiv:1912.04958. Preprint, arXiv, March 23, 2020. https://doi.org/10.48550/arXiv.1912.04958.

Keitel, Anne, Christian Keitel, Mohsen Alavash, et al. "Brain Rhythms in Cognition -- Controversies and Future Directions." arXiv:2507.15639. Preprint, arXiv, July 21, 2025. https://doi.org/10.48550/arXiv.2507.15639.

Leopold, David A., and Gillian Rhodes. "A Comparative View of Face Perception." *Journal of Comparative Psychology (Washington, D.C.: 1983)* 124, no. 3 (2010): 233–51. https://doi.org/10.1037/a0019460.

Lin, Chin-Hsuan, Tim M. Tierney, Niall Holmes, et al. "Using Optically Pumped Magnetometers to Measure Magnetoencephalographic Signals in the Human Cerebellum." *The Journal of Physiology* 597, no. 16 (2019): 4309–24. https://doi.org/10.1113/JP277899.

Liu, Jia, Alison Harris, and Nancy Kanwisher. "Perception of Face Parts and Face Configurations: An fMRI Study." *Journal of Cognitive Neuroscience* 22, no. 1 (2010): 203–11. https://doi.org/10.1162/jocn.2009.21203.

Maris, Eric, and Robert Oostenveld. "Nonparametric Statistical Testing of EEG- and MEG-Data." *Journal of Neuroscience Methods* 164, no. 1 (2007): 177–90. https://doi.org/10.1016/j.jneumeth.2007.03.024.

Montemurro, Marcelo A., Malte J. Rasch, Yusuke Murayama, Nikos K. Logothetis, and Stefano Panzeri. "Phase-of-Firing Coding of Natural Visual Stimuli in Primary Visual Cortex." *Current Biology: CB* 18, no. 5 (2008): 375–80. https://doi.org/10.1016/j.cub.2008.02.023.

Oruc, Ipek, Benjamin Balas, and Michael S. Landy. "Face Perception: A Brief Journey through Recent Discoveries and Current Directions." *Vision Research*, Face perception: Experience, models and neural mechanisms, vol. 157 (April 2019): 1–9. https://doi.org/10.1016/j.visres.2019.06.005.

Paszke, Adam, Sam Gross, Francisco Massa, et al. "PyTorch: An Imperative Style, High-Performance Deep Learning Library." arXiv:1912.01703. Preprint, arXiv, December 3, 2019. https://doi.org/10.48550/arXiv.1912.01703.

Pedregosa, Fabian, Gaël Varoquaux, Alexandre Gramfort, et al. "Scikit-Learn: Machine Learning in Python." *Journal of Machine Learning Research* 12, no. 85 (2011): 2825–30.

Popov, Tzvetan, Gregory A. Miller, Brigitte Rockstroh, and Nathan Weisz. "Modulation of α Power and Functional Connectivity during Facial Affect Recognition." Articles. *Journal of Neuroscience* 33, no. 14 (2013): 6018–26. https://doi.org/10.1523/JNEUROSCI.2763-12.2013.

Rossion, Bruno. "Understanding Individual Face Discrimination by Means of Fast Periodic Visual Stimulation." *Experimental Brain Research* 232, no. 6 (2014): 1599–621. https://doi.org/10.1007/s00221-014-3934-9.

Rossion, Bruno, and Talia L. Retter. "Holistic Face Perception: Mind the Gap!" *Visual Cognition* 23, no. 3 (2015): 379–98. https://doi.org/10.1080/13506285.2014.1001472.

Sauseng, Paul, and Wolfgang Klimesch. "What Does Phase Information of Oscillatory Brain Activity Tell Us about Cognitive Processes?" *Neuroscience and*

Biobehavioral Reviews 32, no. 5 (2008): 1001–13. https://doi.org/10.1016/j.neubiorev.2008.03.014.

Seymour, Robert A., Nicholas Alexander, Stephanie Mellor, et al. "Interference Suppression Techniques for OPM-Based MEG: Opportunities and Challenges." *NeuroImage* 247 (February 2022): 118834. https://doi.org/10.1016/j.neuroimage.2021.118834.

Sollfrank, Teresa, Oona Kohnen, Peter Hilfiker, et al. "The Effects of Dynamic and Static Emotional Facial Expressions of Humans and Their Avatars on the EEG: An ERP and ERD/ERS Study." *Frontiers in Neuroscience* 15 (April 2021). https://doi.org/10.3389/fnins.2021.651044.

Symons, Ashley E., Wael El-Deredy, Michael Schwartze, and Sonja A. Kotz. "The Functional Role of Neural Oscillations in Non-Verbal Emotional Communication." *Frontiers in Human Neuroscience* 10 (May 2016). https://doi.org/10.3389/fnhum.2016.00239.

Tierney, Tim M., Nicholas Alexander, Stephanie Mellor, et al. "Modelling Optically Pumped Magnetometer Interference in MEG as a Spatially Homogeneous Magnetic Field." *NeuroImage* 244 (December 2021): 118484. https://doi.org/10.1016/j.neuroimage.2021.118484.

Virtanen, Pauli, Ralf Gommers, Travis E. Oliphant, et al. "SciPy 1.0: Fundamental Algorithms for Scientific Computing in Python." *Nature Methods* 17, no. 3 (2020): 261–72. https://doi.org/10.1038/s41592-019-0686-2.

Wang, Yifeng, Xinju Huang, Xuezhi Yang, et al. "Low Frequency Phase-Locking of Brain Signals Contribute to Efficient Face Recognition." *Neuroscience* 422 (December 2019): 172–83. https://doi.org/10.1016/j.neuroscience.2019.10.024.

Xu, Wei, Bingjiang Lyu, ..., and Jia-Hong Gao. "Decoding the Temporal Structures and Interactions of Multiple Face Dimensions Using OPM-MEG." Openneuro, 2025. https://doi.org/10.18112/OPENNEURO.DS005107.V2.0.0.

Xu, Wei, Pan Liao, Miao Cao, David J. White, Bingjiang Lyu, and Jia-Hong Gao. "Facilitating Cognitive Neuroscience Research with 80-Sensor Optically Pumped Magnetometer Magnetoencephalography (OPM-MEG)." *NeuroImage* 311 (May 2025): 121182. https://doi.org/10.1016/j.neuroimage.2025.121182.

Xu, Wei, Bingjiang Lyu, Xingyu Ru, et al. "Decoding the Temporal Structures and Interactions of Multiple Face Dimensions Using Optically Pumped Magnetometer Magnetoencephalography (OPM-MEG)." *The Journal of Neuroscience* 44, no. 47 (2024): e2237232024. https://doi.org/10.1523/JNEUROSCI.2237-23.2024.

Yin, Zhongliang, Ying Wang, Minghao Dong, Yubo Wang, Shenghan Ren, and Jimin Liang. "Short-Range and Long-Range Neuronal Oscillatory Coupling in Multiple Frequency Bands during Face Perception." *International Journal of Psychophysiology* 152 (June 2020): 26–35. https://doi.org/10.1016/j.ijpsycho.2020.04.003.

Young, Calvin K., and Jos J. Eggermont. "Coupling of Mesoscopic Brain Oscillations: Recent Advances in Analytical and Theoretical Perspectives." *Progress in Neurobiology* 89, no. 1 (2009): 61–78. https://doi.org/10.1016/j.pneurobio.2009.06.002.

Appendix

Appendix 1: Stimuli

Full table of all 64 different faces.

Appendix 2: Descriptive list of the stimulus

1. asian, young, male, neutral face (slight smile)
2. asian, middle aged, male, neutral face (slight frown)
3. asian, young, male, neutral face (slight smile)
4. asian, middle aged, male, neutral face (slight smile)
5. asian, young/middle aged, male, emotional face: Smile
6. asian, young, male, emotional face: smile
7. asian, young, male, emotional face: smile
8. asian, young, male, emotional face: smile
9. asian, old, male, neutral face: slight open mouth. Glasses
10. asian, old, male, neutral face: slight open mouth. Glasses
11. asian, old, male, neutral face: slight frown
12. asian, old, male, neutral face: slight open mouth
13. asian, old, male, emotional face: very happy, big smile. slight open mouth

14. asian, old, male, emotional face: happy, smile
15. asian, old, male, emotional face: very happy, big smile. slight open mouth
16. asian, old, male, emotional face: happy, smile
17. asian, young, female, neutral face
18. asian, young, female, neutral face
19. asian, young/middle aged, female, neutral face
20. asian, young, female, neutral face
21. asian, young, female, emotional face: smile
22. asian, young, female, emotional face: smile
23. asian, young, female, emotional face: smile
24. asian, young/middle aged, female, emotional face: smile
25. asian, old, female, neutral face
26. asian, old, female, neutral face
27. asian, old, female, neutral face
28. asian, old, female, neutral face. slight open mouth
29. asian, old, female, emotional face: smile
30. asian, old, female, emotional face: smile
31. asian, old, female, emotional face: smile
32. asian, old, female, emotional face: smile
33. caucasian/white, young, male, neutral face
34. caucasian/white, young, male, neutral face
35. caucasian/white, young, male, neutral face
36. caucasian/white, young, male, neutral face
37. caucasian/white, young/middle aged, male, emotional face: smile
38. caucasian/white, young, male, emotional face: smile
39. caucasian/white, young, male, emotional face: smile
40. caucasian/white, young, male, emotional face: smile
41. caucasian/white, old, male, neutral face
42. caucasian/white, old, male, neutral face
43. caucasian/white, old, male, neutral face. glasses
44. caucasian/white, old, male, neutral face
45. caucasian/white, old, male, emotional face: smile
46. caucasian/white, old, male, emotional face: smile
47. caucasian/white, old, male, emotional face: smile. glasses
48. caucasian/white, old, male, emotional face: smile
49. caucasian/white, young, female, neutral face
50. caucasian/white, young, female, neutral face
51. caucasian/white, young, female, neutral face
52. caucasian/white, young, female, neutral face
53. caucasian/white, young, female, emotional face: smile
54. caucasian/white, young, female, emotional face: smile
55. caucasian/white, young, female, emotional face: smile
56. caucasian/white, young, female, emotional face: smile
57. caucasian/white, old, female, neutral face

58. caucasian/white, old, female, neutral face
59. caucasian/white, old, female, neutral face
60. caucasian/white, old, female, neutral face
61. caucasian/white, old, female, emotional face: smile
62. caucasian/white, old, female, emotional face: smile
63. caucasian/white, old, female, emotional face: smile
64. caucasian/white, old, female, emotional face: smile

Appendix 3: Sensor positions

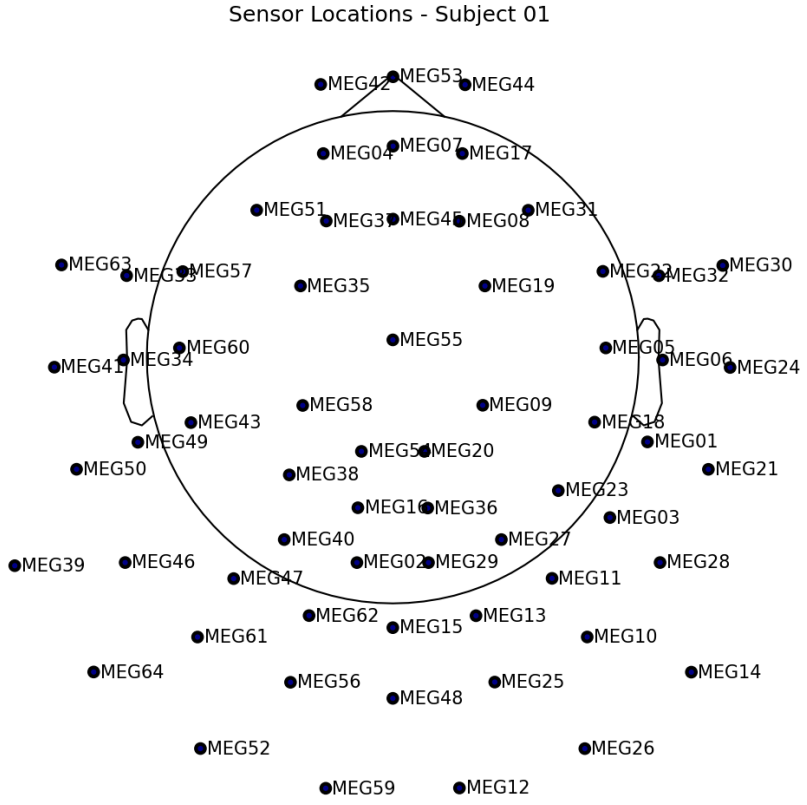

Full-head sensor list: MEG01, MEG02, MEG03, MEG04, MEG05, MEG06, MEG07, MEG08, MEG09, MEG10, MEG11, MEG12, MEG13, MEG14, MEG15, MEG16, MEG17, MEG18, MEG19, MEG20, MEG21, MEG22, MEG23, MEG24, MEG25, MEG26, MEG27, MEG28, MEG29, MEG30, MEG31, MEG32, MEG33, MEG34, MEG35, MEG36, MEG37, MEG38, MEG39, MEG40, MEG41, MEG42, MEG43, MEG44, MEG45, MEG46, MEG47, MEG48, MEG49, MEG50, MEG51, MEG52, MEG53, MEG54, MEG55, MEG56, MEG57, MEG58, MEG59, MEG60, MEG61, MEG62, MEG63, MEG64.

List of **posterior** channels (ROI) used for analysis: *MEG12, MEG23, MEG25, MEG26, MEG28, MEG39, MEG48, MEG49, MEG50, MEG54, MEG59*

Appendix 4: Examples of PSD before / after preprocessing

Appendix 5: Total trials across subject between conditions (Emotional vs Neutral)

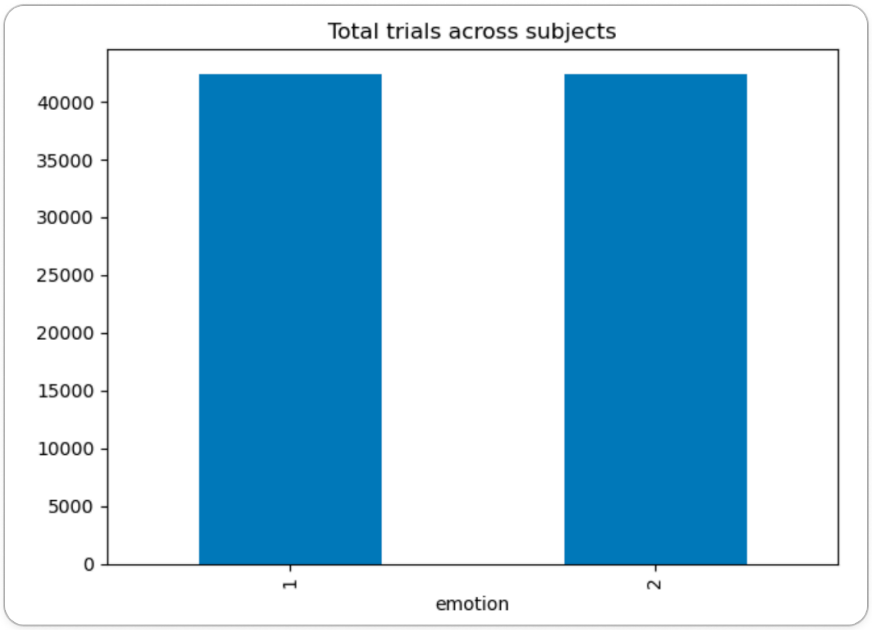

emotion	1	2
sub-01	2510	2520
sub-02	758	758
sub-03	2520	2514
sub-04	2516	2525
sub-06	2507	2501
sub-07	2460	2473
sub-08	1267	1256
sub-09	2531	2523
sub-10	1001	991
sub-11	1737	1740
sub-13	2512	2510
sub-14	2507	2496
sub-15	1260	1267
sub-16	1252	1248
sub-17	2514	2504
sub-18	1263	1255
sub-19	2512	2515
sub-20	2496	2502
sub-21	2519	2516
sub-22	1252	1244
sub-23	2501	2505

Appendix 6: Extra analysis plots

H1:

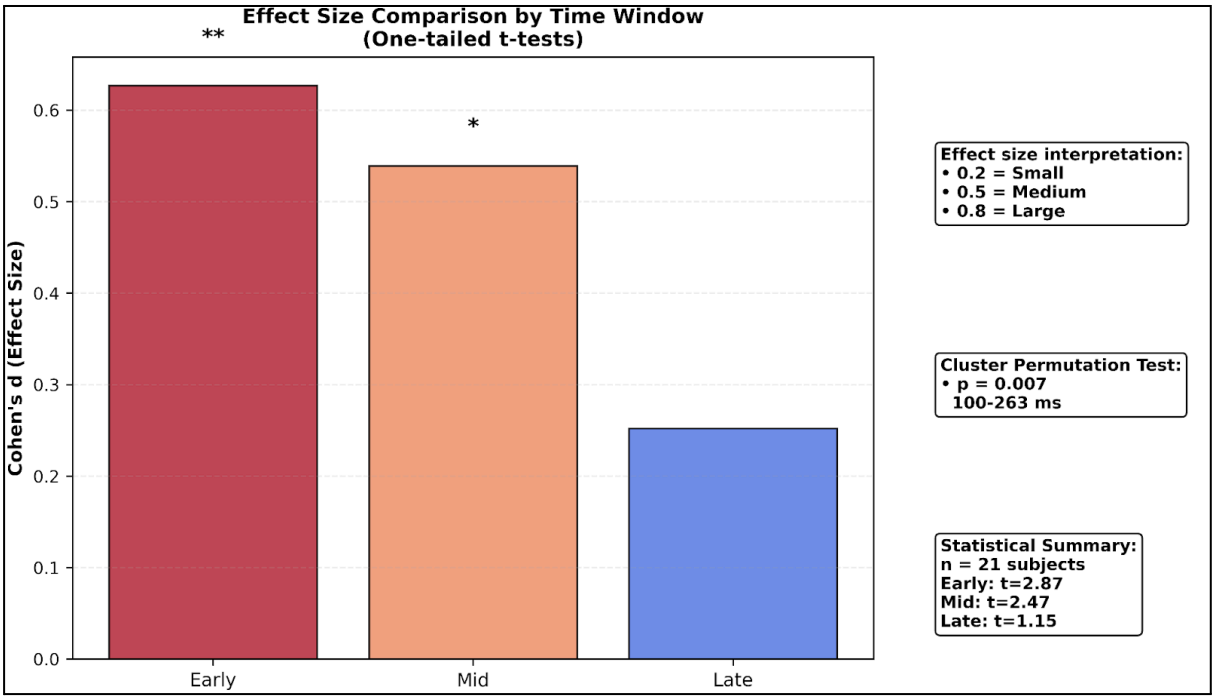

Figure 15: Effect Size Comparison by Time Window (One-tailed t-tests)
Comparison of Cohen's d effect sizes across time windows with cluster permutation test results and statistical annotations moved to sidebar. Early window shows medium-to-large effect (d=0.627), mid window shows

medium effect (d=0.539), late window shows small, non-significant effect (d=0.252). Cluster permutation test results: significant cluster p=0.007, spanning 100-263 ms. Effect size interpretation: d=0.2 (small), d=0.5 (medium), d=0.8 (large). All statistical details provided in sidebar.

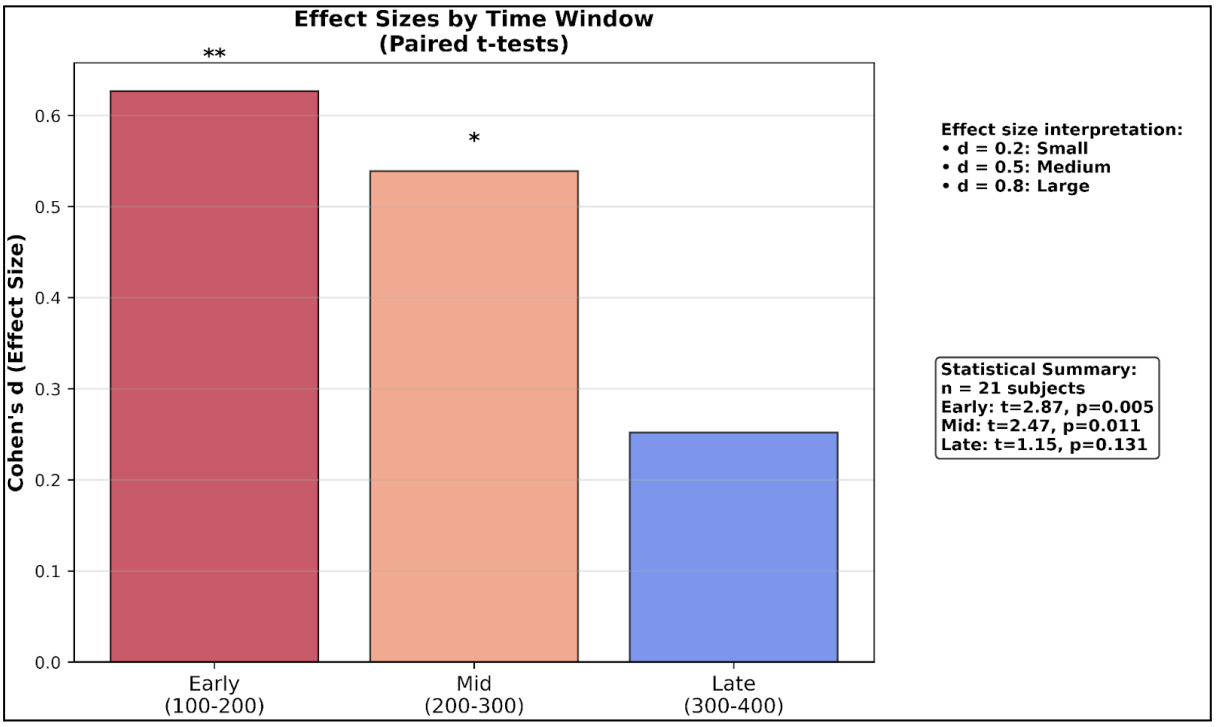

Figure 16: Effect Sizes by Time Window (Paired t-tests)
Cohen's d effect sizes for theta power differences in three a priori time windows with statistical annotations moved to sidebar. Bar colors correspond to time windows: early (100-200 ms, dark red), mid (200-300 ms, muted red), late (300-400 ms, steel blue). Statistical results: Early window: d=0.627, t(20)=2.872, p=0.005*; Mid window: d=0.539, t(20)=2.470, p=0.011*; Late window: d=0.252, t(20)=1.155, p=0.131. Error bars omitted as Cohen's d represents standardized effect size. Effect size interpretation guide included in sidebar.

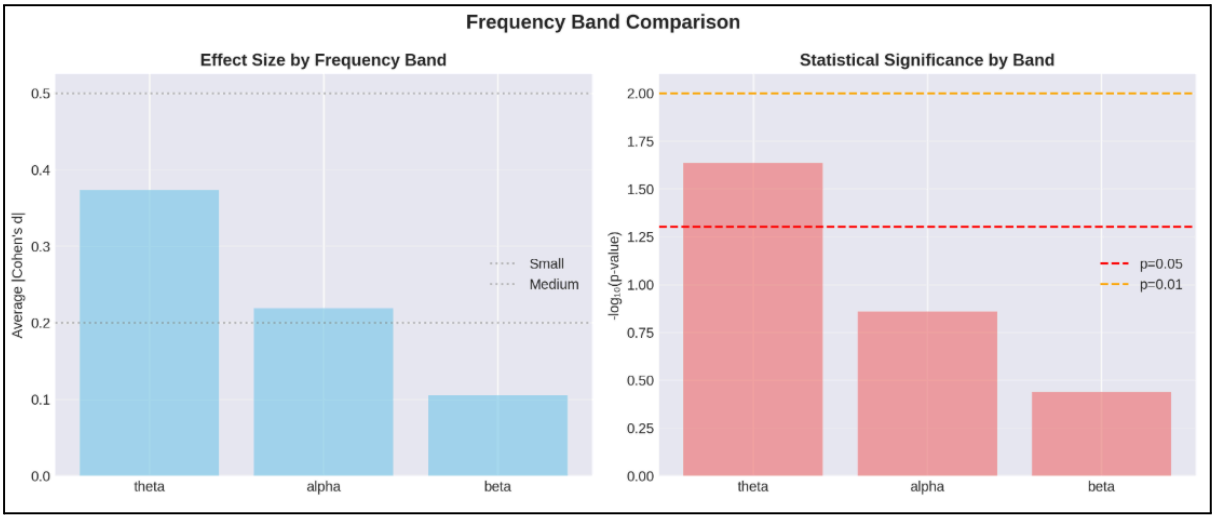

Figure 17. Frequency Band Comparison. (A) Average absolute effect size (|Cohen's *d*|) for each frequency band. (B) Statistical significance for each band, represented as the minimum p-value (transformed to -log10) across its three time windows. The dashed lines indicate common significance thresholds.

The specificity of the emotional modulation to the theta rhythm is further emphasized by comparing effects across frequency bands in Figure 17. Panel A illustrates the average magnitude of effects for each band, while Panel B presents their statistical significance. Analysis of other frequency bands showed no statistically significant effects. In the alpha band (8-12 Hz), patterns were inconsistent, with a non-significant increase early ($p = .138$, $d = 0.24$) and a non-significant decrease later ($p = .901$, $d = -0.29$). The beta band (13-30 Hz) showed no reliable differences (all $p > .36$, $|d| < 0.13$).

The specificity of the modulation to the theta rhythm, with no reliable effects in the alpha or beta bands, argues against a general, non-specific increase in cortical arousal. Instead, it supports models proposing a privileged role for theta oscillations in the initial orienting of attention toward emotional significance and the coordination of neural assemblies for efficient processing (Symons et al., 2016). This is consistent with the framework proposed by Keitel et al. (2025), where theta rhythms increase when the visual system encounters affectively significant stimuli. The broad topographic distribution of the effect further supports the notion of a network-level response, integral for binding the multidimensional features of a face into a coherent percept across the distributed core and extended face-processing systems (Haxby et al., 2000). This result solidifies theta power as a robust electrophysiological signature of early emotional salience detection in face perception.